Title	An efficient hierarchical multiscale finite element method for stokes equations in slowly varying media
Author(s)	Brown, Donald L.; Efendiev, Yalchin; Hoang, Viet Ha
Citation	Brown, D. L., Efendiev, Y., & Hoang, V. H. (2013). An Efficient Hierarchical Multiscale Finite Element Method for Stokes Equations in Slowly Varying Media. Multiscale Modeling & Simulation, 11(1), 30-58.
Date	2013
URL	http://hdl.handle.net/10220/18461
Rights	© 2013 Society for Industrial and Applied Mathematics. This paper was published in Multiscale Modeling & Simulation and is made available as an electronic reprint (preprint) with permission of Society for Industrial and Applied Mathematics. The paper can be found at the following official DOI: [http://dx.doi.org/10.1137/110858525]. One print or electronic copy may be made for personal use only. Systematic or multiple reproduction, distribution to multiple locations via electronic or other means, duplication of any material in this paper for a fee or for commercial purposes, or modification of the content of the paper is prohibited and is subject to penalties under law.

© 2013 Society for Industrial and Applied Mathematics

AN EFFICIENT HIERARCHICAL MULTISCALE FINITE ELEMENT METHOD FOR STOKES EQUATIONS IN SLOWLY VARYING MEDIA*

DONALD L. BROWN†, YALCHIN EFENDIEV‡, AND VIET HA HOANG§

Abstract. Direct numerical simulation (DNS) of fluid flow in porous media with many scales is often not feasible, and an effective or homogenized description is more desirable. To construct the homogenized equations, effective properties must be computed. Computation of effective properties for nonperiodic microstructures can be prohibitively expensive, as many local cell problems must be solved for different macroscopic points. In addition, the local problems may also be computationally expensive. When the microstructure varies slowly, we develop an efficient numerical method for two scales that achieves essentially the same accuracy as that for the full resolution solve of every local cell problem. In this method, we build a dense hierarchy of macroscopic grid points and a corresponding nested sequence of approximation spaces. Essentially, solutions computed in high accuracy approximation spaces at select points in the the hierarchy are used as corrections for the error of the lower accuracy approximation spaces at nearby macroscopic points. We give a brief overview of slowly varying media and formal Stokes homogenization in such domains. We present a general outline of the algorithm and list reasonable and easily verifiable assumptions on the PDEs, geometry, and approximation spaces. With these assumptions, we achieve the same accuracy as the full solve. To demonstrate the elements of the proof of the error estimate, we use a hierarchy of macro–grid points in $[0,1]^2$ and finite element (FE) approximation spaces in $[0,1]^2$. We apply this algorithm to Stokes equations in a slowly porous medium where the microstructure is obtained from a reference periodic domain by a known smooth map. Using the arbitrary Lagrangian–Eulerian (ALE) formulation of the Stokes equations (cf. [G. P. Galdi and R. Rannacher, *Fundamental Trends in Fluid-Structure Interaction*, Contemporary Challenges in Mathematical Fluid Dynamics and Its Applications 1, World Scientific, Singapore, 2010]), we obtain modified Stokes equations with varying coefficients in the periodic domain. We show that the algorithm can be utilized in this setting. Finally, we implement the algorithm on the modified Stokes equations, using a simple stretch deformation mapping, and compute the effective permeability. We show that our efficient computation is of the same order as the full solve.

Key words. Stokes flow homogenization, multilevel finite elements, fluid-structure interaction, arbitrary Lagrange–Eulerian

AMS subject classifications. 74Qxx, 74Q15, 74S05, 76D07, 74F10

DOI. 10.1137/110858525

1. Introduction. Understanding flow in porous media has wide ranging applications in various areas of science and engineering. A large portion of these applications lies in the field of subsurface simulation. For example, in petroleum engineering, flow information is used to provide economically efficient production strategies. In envi-

†Corresponding author. Department of Mathematics, Texas A&M University, College Station, TX 77843 (browdr@neo.tamu.edu).

‡Department of Mathematics, Texas A&M University, College Station, TX 77843 (efendiev@ math.tamu.edu). This author's work was partially supported by the US Army (62151-MA), the DOE, and the NSF (DMS 0934837, DMS 0724704, and DMS 0811180).

§Division of Mathematical Sciences, School of Physical and Mathematical Sciences, Nanyang Technological University, Singapore 637371, Singapore (VHHOANG@ntu.edu.sg).

ronmental engineering, understanding subsurface water flow can be used to predict contaminant transport in aquifers. In most cases, porous media exhibit heterogeneous microstructure and have many scales. This makes direct numerical simulation (DNS) prohibitively expensive. More specifically, the pore size is much smaller than the domain of interest, and so effective equations are more desirable. In these situations, homogenization or averaging techniques are employed to understand the physics on an effective scale.

Traditionally, these methods rely heavily on the medium of interest having a purely periodic structure. However, there are many multiscale and multiphysical problems in which an initially periodic medium, through some coupled process, breaks the periodicity. This is often achieved in a slowly varying way, where the pore-space of two neighboring representative volume elements (RVEs) differs very little. Examples of such processes include fluid-structure interaction (FSI), where mechanical deformation, driven by normal stresses at the fluid-solid interface, breaks periodicity in a slowly varying way; cf. [6, 7, 19]. In the case of concrete carbonation, chemical degradation breaks down the periodic microstructure (cf. [17, 18]), and in industrial filtration, deposition of contaminants yields a slowly varying pore-space; cf. [16].

In this work we consider creeping flow of an incompressible Newtonian fluid in a microstructure that is slowly varying. The governing equations for these types of flows are given by the Stokes equations [21]. We develop a novel and efficient two-scale finite element method (FEM) to compute solutions to the auxiliary cell equations. These cell problems relate the microscale information to the macroscale or effective description. In turn, we are able to construct a numerical approximation to the homogenized equations in slowly varying geometries. In this method, we are able to reuse previously computed information from nearby cell equations to obtain a more accurate solution at a reduced computational cost. The main goal of our paper is to show that we obtain the same order of accuracy with our algorithm as the much more costly full solve.

In the event that the media are periodic, analytical techniques and computational algorithms for Stokes homogenization are well studied. Using the method of two-scale asymptotic expansion [9, 10, 20], the authors develop a formal justification for the homogenization of Stokes equations in perforated domains. First, auxiliary cell equations are deduced; then, after averaging, the solutions are used to construct the homogenized Darcy equation [8]. In the periodic setting, the cell equations completely uncouple from macro–scale variables and depend only on the cell pore geometry. This fact, along with periodicity, results in a single set of cell equations that must be computed to construct the homogenized equations. In slowly varying media this is not the case; as the geometry changes, a new set of cell equations must be calculated. This is often also true for elliptic problems with highly oscillatory coefficients [2]. For example, in two-scale diffusion problems, the diffusivity tensor may depend on both macro- and microscales. For each macroscopic point a corresponding set of cell equations must be computed.

In practice, we cannot compute a set of cell equations for each macroscopic point. In [7], the authors develop a moving averages homogenization algorithm, a numerical technique for constructing the homogenized Darcy equation in slowly varying media. By computing the set of cell problems at many select macroscopic points using a standard FEM and interpolating the result, a numerical approximation to the homogenized equation is obtained. This approach, although successful in its task, can be improved upon in a number of ways. Each of the cell equations is computed using the same order of accuracy and must be remeshed for each unique geometry. This

can be computationally expensive, especially in cases where the cell geometry is very complicated. Even though the geometry is slowly varying and there is little change from RVE to RVE, information from nearby cells cannot be reused without sampling errors from interpolating solutions with differing meshes. Since the geometries vary little, there is some redundancy in recalculating cell problems in nearby RVEs. In this work, we develop techniques to circumvent these difficulties.

The idea of the algorithm is as follows. We first develop an algorithm that yields a hierarchy of grids, with specified qualities, in the macroscopic variable. Traditionally, we would solve a set of cell problems at all these macroscopic grid points with the same accuracy as in the method of moving averages [7]. In our proposed framework, we build a corresponding nested collection of finite element (FE) approximation spaces with varying orders of accuracy to compute cell equations. With some macrogrids we compute very accurate cell solutions, and with more refined macrogrids (closer grid spacing) we compute cell solutions with less accuracy. We use local information from nearby higher accuracy solutions known as "right-hand-side data" to correct the lower accuracy solves. These ideas have been used successfully for elliptic problems. In the case where a high-dimensional homogenized equation is available, the sparse tensor product discretization approach developed in [15] computes the solution to the effective equation and the corrector with a complexity essentially equal to that for solving a single macroscopic PDE and achieves accuracy essentially equal to that for the full solve, without forming the effective equation explicitly. As for the Stokes equations, for the elliptic problem considered in [15], if the effective coefficient is of interest, it can be computed efficiently with much reduced complexity by our method. This method is a special case of the wide class of heterogeneous multiscale methods (HMMs), where local properties are used to update macroscale phenomena. For more on these topics we refer the reader to [1] and the references therein.

Often, slowly varying media arise from coupled physical processes. In this work, we assume the mapping from the initial periodic (reference) configuration to the slowly varying (current) configuration is known. For example, in iterative FSI, fluid equations are solved, and then normal stresses at the interface are passed to the solid mechanics equations. The displacement of the solid is computed, and fluid equations are solved again in the newly deformed domain; cf. [19]. At each iteration step, the deformation from the reference to the current configuration is computed by composing displacements of each iteration. With this information, we are able to reformulate the Stokes equations in a slowly varying domain to modified Stokes equations with tensor coefficients in the initial periodic domain. In the context of FSI, this reformulation is referred to as the arbitrary Lagrange–Eulerian (ALE) formulation of the Stokes equations; cf. [12, 13]. The periodic ALE formulation allows us to construct a nested collection of FE spaces. The geometry does not change, but instead the tensor coefficients vary. In this formulation, we are able to prove with reasonable and easily verifiable assumptions that our algorithm produces essentially the same order of accuracy as the full solve with much reduced complexity.

The organization of the paper is as follows. First, in section 2 we motivate the need for an efficient multiscale algorithm in slowly varying media. We begin by giving a summary of formal homogenization of Stokes equations in such media. This will serve to introduce terminology used throughout the work and highlight advantages of reformulating the problem in the ALE formulation. Then, an overview of the solution approach and computational algorithm is presented in general terms. In section 3 we outline physically reasonable and easily verifiable abstract mathematical assumptions on the microstructure geometry, variational equations, and FE approximation spaces.

These assumptions will guarantee that our algorithm has the same order of accuracy as the full solve, but at less computational cost. We prove this for a two-dimensional hierarchy of macrogrids to illustrate the main ideas of the proof. Then, in section 4 we reformulate the Stokes equations from the slowly varying geometry to the periodic ALE formulation. We verify that the abstract assumptions outlined in section 3 hold, assuming the geometry is slowly varying. Hence, our efficient multiscale algorithm will be applicable in this setting. Finally, to demonstrate the ideas and effectiveness of the algorithm, in section 5 we apply our algorithm to a constructed example where initially periodic media with square inclusions are deformed via a horizontal stretch. We show that our algorithm is the same order of accuracy as the full fine mesh solve by comparing permeabilities or averaged cell velocity solutions.

2. Background and overview of the algorithm. In this section we give a brief exposition of slowly varying domains, formal Stokes homogenization in such media, and an overview of our efficient multiscale FE algorithm. We introduce periodic perforated domains, and then, after applying a mapping, we obtain the slowly varying domain. This mapping is an a priori known quantity computed from another coupled process such as FSI deformation, chemical degradation, etc. [18, 19]. The homogenization background will serve to motivate our algorithm and give definitions to general terminology used throughout the paper. We follow the presentation of this material given in [7], where when using two-scale expansions in slowly varying domains, homogenization results are obtained. To this end, we introduce the fine-scale Stokes operator, and then via formal two-scale asymptotic expansions [20], we arrive at the auxiliary cell operator. From here we can construct the homogenized equations.

We are then in a position to give an overview for our algorithm. First, we highlight the challenges in the numerical homogenization of the equations presented in section 2.1. The primary challenge is that, due to the changing pore geometry, we must solve many sets of cell problems at various points in the domain. A synopsis of the algorithm approach is given. We outline the requisite properties of the hierarchy of macrogrids and corresponding nested sequence of FE approximation spaces. We then state the procedure required to obtain the desired order of accuracy.

2.1. Slowly varying media and homogenization of Stokes flow. We begin with some basic notation. Let the macroscopic domain Ω be an open bounded subset of $\mathbb{R}^d$. We assume that the domain is periodically perforated by an open solid microstructure denoted by $\mathcal{S}_\varepsilon$. The solid surrounds a connected fluid pore-space denoted by $\mathcal{F}_\varepsilon$. That is, $\Omega = \mathcal{F}_\varepsilon \cup \mathcal{S}_\varepsilon$ and $\mathcal{F}_\varepsilon \cap \mathcal{S}_\varepsilon = \emptyset$. The interface between the two media is denoted by $\Gamma_\varepsilon = \bar{\mathcal{F}}_\varepsilon \cap \bar{\mathcal{S}}_\varepsilon$. Furthermore, we assume that the media have an additional structure. The two domains are decomposed into a set of unit cells $\varepsilon \left\{ Y_{\mathcal{F}}^i \right\}_{i=1}^{N}$ and $\varepsilon \left\{ Y_{\mathcal{S}}^i \right\}_{i=1}^{N}$, respectively, and ε is the characteristic pore size. That is, $Y_{\mathcal{S}}^i$ and $Y_{\mathcal{F}}^i$, $i = 1, \ldots, N$, are unit-sized domains and

$$(1) \qquad \mathcal{F}_\varepsilon = \left(\bigcup_{i=1}^{N} \varepsilon Y_{\mathcal{F}}^i \right) \cap \Omega, \qquad \mathcal{S}_\varepsilon = \left(\bigcup_{i=1}^{N} \varepsilon Y_{\mathcal{S}}^i \right) \cap \Omega.$$

Since the domain is assumed to be periodic, each of the cells differs only by a translation. That is, $Y_{\mathcal{F}}^i = Y_{\mathcal{F}} + k_i$ and $Y_{\mathcal{S}}^i = Y_{\mathcal{S}} + k_i$, where $k_i \in \mathbb{Z}^d$ corresponds to the ith cell. We denote the entire unit cell by $Y = Y_{\mathcal{F}} \cup Y_{\mathcal{S}}$ and the cell interface Y_Γ.

Let $\widetilde{\mathbf{x}}_\varepsilon : \Omega \to \widetilde{\Omega}_\varepsilon$ be a smooth map of the periodic domain to the deformed domain $\widetilde{\Omega}_\varepsilon$. Consequently, we may define the deformed fluid, solid, and interface as
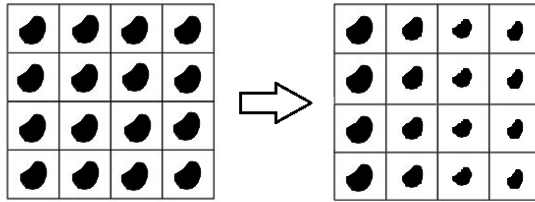
FIG. 1. *Mapping from periodic* $\Omega = \mathcal{F}_\varepsilon \cup \mathcal{S}_\varepsilon$ *to slowly varying* $\widetilde{\Omega}_\varepsilon = \widetilde{\mathcal{F}}_\varepsilon \cup \widetilde{\mathcal{S}}_\varepsilon$ *by* $\widetilde{\mathbf{x}}_\varepsilon$. *The fluid and solid are white and black, respectively, in both domains.*

$\widetilde{\mathcal{F}}_\varepsilon = \widetilde{\mathbf{x}}_\varepsilon(\mathcal{F}_\varepsilon)$, $\widetilde{\mathcal{S}}_\varepsilon = \widetilde{\mathbf{x}}_\varepsilon(\mathcal{S}_\varepsilon)$, and $\widetilde{\Gamma}_\varepsilon = \widetilde{\mathbf{x}}_\varepsilon(\Gamma_\varepsilon)$, respectively. We denote the coordinates of the periodic geometry by x and the slowly varying geometry by $\tilde{x}$. We denote physical quantities in the slowly varying geometry by a $\widetilde{}$. An example of two domains can be seen in Figure 1, where $\Omega = [0,1]^2$ and $\varepsilon = 1/4$. Each unit cell is now deformed, so we define an RVE. For each $\tilde{x} \in \widetilde{\Omega}$ the fluid and solid cell domains contained in an RVE are denoted by $Y_{\widetilde{\mathcal{S}}}^{\tilde{x}}$ and $Y_{\widetilde{\mathcal{F}}}^{\tilde{x}}$, and the interface by $Y_{\widetilde{\Gamma}}^{\tilde{x}}$. The deformation creates a natural correspondence between translated periodic cells and deformed cells. We view the slowly varying RVEs as the image of the mapping $\widetilde{\mathbf{x}}_\varepsilon$ restricted to translated periodic cells. That is, $\varepsilon Y_{\widetilde{\mathcal{F}}}^{\tilde{x}} = \widetilde{\mathbf{x}}_\varepsilon(\varepsilon(Y_\mathcal{F} + k_x))$ and $\varepsilon Y_{\widetilde{\mathcal{S}}}^{\tilde{x}} = \widetilde{\mathbf{x}}_\varepsilon(\varepsilon(Y_\mathcal{S} + k_x))$, where $k_x \in \mathbb{Z}^d$ corresponds to the RVE at $x \in \Omega$ in the periodic domain. Thus, the deformed fluid and solid space are given by

$$\widetilde{\mathcal{F}}_\varepsilon = \bigcup_{\tilde{x} \in \widetilde{\Omega}} \varepsilon Y_{\widetilde{\mathcal{F}}}^{\tilde{x}}, \qquad \widetilde{\mathcal{S}}_\varepsilon = \bigcup_{\tilde{x} \in \widetilde{\Omega}} \varepsilon Y_{\widetilde{\mathcal{S}}}^{\tilde{x}}.$$

Remark. Recalling the formal definition of slowly varying media given in [7], we say a medium is slowly varying if nearby RVE pore geometry differs slightly. More precisely, we say that $\widetilde{\Omega}_\varepsilon$ is slowly varying if the map $\widetilde{\mathbf{x}}_\varepsilon$ is such that if $\tilde{x}, \tilde{x}' \in \widetilde{\Omega}_\varepsilon$ and $\|\tilde{x} - \tilde{x}'\| < O(\varepsilon)$, then

$$|(Y_{\widetilde{\mathcal{F}}}^{\tilde{x}} \cup Y_{\widetilde{\mathcal{F}}}^{\tilde{x}'}) \backslash (Y_{\widetilde{\mathcal{F}}}^{\tilde{x}} \cap Y_{\widetilde{\mathcal{F}}}^{\tilde{x}'})| < O(\varepsilon).$$

In this work, we will need to make more concrete assumptions on the mapping $\widetilde{\mathbf{x}}_\varepsilon$. Indeed, we will require that the mapping and its gradient be sufficiently smooth and Lipschitz continuous with respect to the macroscopic (slow) variables.

It is common practice in applied sciences and engineering applications to use RVEs at many macroscopic points. The RVEs contain a representative sample of small-scale information. At each of these points, local problems are solved. For complex microstructure this can be very computationally expensive. To resolve local flow properties, Stokes equations are solved in the RVEs assuming periodic boundary conditions. These boundary conditions assume that, near a fixed macroscopic point, the microstructure is periodic. Next, we present a formal derivation of this type of procedure by two-scale asymptotic expansions for Stokes flow in slowly varying domains. This will serve to introduce general terminology and motivate our algorithm.

We suppose that we have an incompressible Newtonian fluid in the pore-space with viscosity μ. The fine-scale pressure and velocity are denoted by $\widetilde{p}_\varepsilon$ and $\widetilde{v}_\varepsilon$, respectively. The flow of such a fluid at creeping velocities is governed by the Stokes approximation [21]. The conservation of linear momentum and conservation of mass

then read as

$$-\nabla \widetilde{p}_\varepsilon + \mu \Delta \widetilde{v}_\varepsilon = \widetilde{f} \text{ in } \widetilde{\mathcal{F}}_\varepsilon, \tag{2a}$$

$$\nabla \cdot \widetilde{v}_\varepsilon = 0 \text{ in } \widetilde{\mathcal{F}}_\varepsilon, \tag{2b}$$

and we assume the boundary condition $\widetilde{v}_\varepsilon = 0$ on $\widetilde{\Gamma}_\varepsilon$. For convenience in notation for what follows, we let $\widetilde{\mathcal{L}}_\varepsilon\left(\tilde{x}, \frac{\tilde{x}}{\varepsilon}\right)$ denote the above fine-scale Stokes operator. Using the two-scale expansions first proposed in [9, 10], pressure and velocity are expanded as

$$\widetilde{v}_\varepsilon(\tilde{x}) = \varepsilon^2 \left(\widetilde{v}_0(\tilde{x}, \tilde{y}) + \varepsilon \widetilde{v}_1(\tilde{x}, \tilde{y}) + \cdots\right), \tag{3a}$$

$$\widetilde{p}_\varepsilon(\tilde{x}) = \widetilde{p}_0(\tilde{x}) + \varepsilon \widetilde{p}_1(\tilde{x}, \tilde{y}) + \cdots, \tag{3b}$$

where $\tilde{y} = \tilde{x}/\varepsilon$ is the fast variable and derivatives behave as $\nabla \to \nabla_{\tilde{x}} + \frac{1}{\varepsilon}\nabla_{\tilde{y}}$. The cell problems are now stated for a given spatial position. Fixing $\tilde{x}$ and substituting the expansions (3) into the Stokes equations (2), gathering ε^0 terms in the conservation of linear momentum and ε^1 terms in the incompressibility equation, one obtains

$$-\nabla_{\tilde{y}}\widetilde{p}_1(\tilde{x}, \tilde{y}) + \mu \Delta_{\tilde{y}}\widetilde{v}_0(\tilde{x}, \tilde{y}) = \widetilde{f}(\tilde{x}) + \nabla_{\tilde{x}}\widetilde{p}_0(\tilde{x}) \qquad \text{in } Y_{\widetilde{\mathcal{F}}}^{\tilde{x}}, \tag{4a}$$

$$\nabla_{\tilde{y}} \cdot \widetilde{v}_0(\tilde{x}, \tilde{y}) = 0 \qquad \text{in } Y_{\widetilde{\mathcal{F}}}^{\tilde{x}}, \tag{4b}$$

where $\widetilde{v}_0$ and $\widetilde{p}_1$ are $\tilde{y}$-periodic; we also require $\widetilde{v}_0 = 0$ on $Y_{\widetilde{\Gamma}}^{\tilde{x}}$ and $\langle \widetilde{p}_1 \rangle_{Y^{\tilde{x}}} = 0$. Here, $\langle \cdot \rangle_{Y^{\tilde{x}}}$ is the average over the unit cell centered at $\tilde{x}$ given by

$$\langle \cdot \rangle_{Y^{\tilde{x}}} = \frac{1}{\left|Y^{\tilde{x}}\right|} \int_{Y^{\tilde{x}}} \cdot \, d\tilde{y}. \tag{5}$$

Next, due to linearity of (4) and the right-hand side being a function of the slow variable $\tilde{x}$ only, one has

$$\widetilde{v}_0(\tilde{x}, \tilde{y}) = \widetilde{w}(\tilde{x}, \tilde{y}) \cdot \left(\widetilde{f}(\tilde{x}) + \nabla_{\tilde{x}}\widetilde{p}_0(\tilde{x})\right), \tag{6a}$$

$$\widetilde{p}_1(\tilde{x}, \tilde{y}) = \widetilde{\pi}(\tilde{x}, \tilde{y}) \cdot \left(\widetilde{f}(\tilde{x}) + \nabla_{\tilde{x}}\widetilde{p}_0(\tilde{x})\right), \tag{6b}$$

where $(\widetilde{w}^i(\tilde{x}, \tilde{y}), \widetilde{\pi}^i(\tilde{x}, \tilde{y}))$, $i = 1, \ldots, d$, are the solutions to the auxiliary cell equations

$$-\nabla_{\tilde{y}}\widetilde{\pi}^i + \mu \Delta_{\tilde{y}}\widetilde{w}^i = e_i \text{ in } Y_{\widetilde{\mathcal{F}}}^{\tilde{x}}, \tag{7a}$$

$$\mathrm{div}_{\tilde{y}}\left(\widetilde{w}^i\right) = 0 \text{ in } Y_{\widetilde{\mathcal{F}}}^{\tilde{x}}, \tag{7b}$$

where $\widetilde{w}^i$ and $\widetilde{\pi}^i$ are $\tilde{y}$-periodic, $\widetilde{w}^i = 0$ on $Y_{\widetilde{\Gamma}}^{\tilde{x}}$, and $\langle \pi^i \rangle_{Y^{\tilde{x}}} = 0$. Here, e_i is the ith standard unit vector in $\mathbb{R}^d$. Again, for convenience in presentation, in the following we denote the above Stokes cell operator as $\widetilde{\mathcal{L}}_{\tilde{y}}(\tilde{x})$. Now, to relate these cell problems to the the classical Darcy equation [8], one inserts (3a) into the conservation of mass of the fine scale operator (2) and, by collecting ε^2 terms, we obtain

$$\nabla_{\tilde{x}} \cdot \widetilde{v}_0 + \nabla_{\tilde{y}} \cdot \widetilde{v}_1 = 0 \text{ in } \widetilde{\mathcal{F}}_\varepsilon. \tag{8}$$

We fix $\tilde{x}$ and integrate over the cell $Y_{\widetilde{\mathcal{F}}}^{\tilde{x}}$. Using the divergence theorem, the fact that $\widetilde{v}_1$ has zero trace on $Y_{\Gamma}^{\tilde{x}}$, $\tilde{y}$-periodicity, and (6a), one obtains the homogenized macroscopic equation of Darcy type

$$\nabla_{\tilde{x}} \cdot \left(\widetilde{\mathbf{K}}(\tilde{x}) \left(\nabla_{\tilde{x}}\widetilde{p}_0(\tilde{x}) + \widetilde{f}(\tilde{x})\right)\right) = 0 \text{ in } \widetilde{\Omega}, \tag{9}$$

where the $\tilde{x}$-dependent permeability is defined as $\widetilde{K}_{ij}(\tilde{x}) := \int_{Y_{\widetilde{\mathcal{F}}}^{\tilde{x}}} \widetilde{w}^{ij}(\tilde{x}, \tilde{y}) d\tilde{y}$ and we define the Darcy velocity $\widetilde{\xi} = \widetilde{\mathbf{K}}(\tilde{x})(\widetilde{f}(\tilde{x}) + \nabla_{\tilde{x}} \widetilde{p}_0(\tilde{x}))$. We require the boundary condition $\widetilde{\xi} \cdot \widetilde{\nu} = 0$ on $\partial \widetilde{\Omega}$, where $\widetilde{\nu}$ is the outward normal. In what follows, we denote the above homogenized operator as $\widetilde{\mathcal{L}}(\tilde{x})$. Note that in the periodic setting we have only one cell geometry and need only compute one set of cell equations (7). Thus, $\widetilde{\mathbf{K}}(\tilde{x}) = \widetilde{\mathbf{K}}$ is constant and does not depend on the slow variable.

Remark. In addition, we require that the mapping $\widetilde{\mathbf{x}}_\varepsilon$ be smooth enough so that the asymptotic expansions (3) will yield correct cell equations (4) and that the permeability $\widetilde{\mathbf{K}}(\tilde{x})$ is a sufficiently smooth enough function of the slow variable $\tilde{x}$. Formally speaking, the map does not change the microstructure from neighboring RVEs in a significant way and varies slowly.

2.2. Overview of the algorithm. The main goal of employing the two-scale asymptotic expansion is to obtain effective homogenized macroscopic equations $\widetilde{\mathcal{L}}(\tilde{x})$ of the fine-scale equations $\widetilde{\mathcal{L}}_\varepsilon\left(\tilde{x}, \frac{\tilde{x}}{\varepsilon}\right)$, given here by (9) and (2), respectively. Often, due to scale disparity and complex pore geometry, computing solutions of the fine-scale equations by DNS is prohibitively expensive. In numerical homogenization, we wish to construct an approximation to the homogenized equations $\widetilde{\mathcal{L}}(\tilde{x})$ by computing solutions to auxiliary cell equations $\widetilde{\mathcal{L}}_{\tilde{y}}(\tilde{x})$, given here by (7). In the periodic setting, this is inexpensive, as $\widetilde{\mathcal{L}}_{\tilde{y}}(\tilde{x}) = \widetilde{\mathcal{L}}_{\tilde{y}}$. In this section, we outline an efficient multiscale algorithm to compute the homogenized equations in slowly varying geometries.

The solution approach can be summarized as follows. Since we are given the mapping $\widetilde{\mathbf{x}}_\varepsilon$ a priori, we use it to reformulate Stokes equations in the periodic ALE formulation [12, 13]. This process transfers the information of the slowly varying geometry to tensor coefficients of the modified Stokes equations. Then, we apply the two-scale asymptotic expansion homogenization technique to the modified Stokes equations $\mathcal{L}_\varepsilon\left(x, \frac{x}{\varepsilon}\right)$. This yields the cell equations $\mathcal{L}_y(x)$ and, subsequently, the homogenized equations $\mathcal{L}(x)$. We are then able work in fixed cell domains $Y_{\mathcal{F}}$ as opposed to $Y_{\widetilde{\mathcal{F}}}^{\tilde{x}}$ for many values of $\tilde{x}$. This fixed domain approach simplifies the analysis and allows for information from nearby RVEs to be used in an effective way. The approach may be summed up in the following diagram:

$$\widetilde{\mathcal{L}}_\varepsilon\left(\tilde{x}, \frac{\tilde{x}}{\varepsilon}\right) \xrightarrow{\text{Two-Scale}} \widetilde{\mathcal{L}}_{\tilde{y}}(\tilde{x}) \xrightarrow{\text{Averaging}} \widetilde{\mathcal{L}}(\tilde{x})$$

$$\Big\downarrow \text{Reformulate Equations in Periodic Domain} \Big\uparrow$$

$$\mathcal{L}_\varepsilon\left(x, \frac{x}{\varepsilon}\right) \xrightarrow{\text{Two-Scale}} \mathcal{L}_y(x) \xrightarrow{\text{Averaging}} \mathcal{L}(x).$$

We present explicit expressions for the operators $\mathcal{L}_\varepsilon\left(x, \frac{x}{\varepsilon}\right)$, $\mathcal{L}_y(x)$, and $\mathcal{L}(x)$ in section 4, and in the appendix we derive the equations by two-scale expansion.

First, we give some mathematical preliminaries. We keep the presentation abstract in the interest of generality because the methods here may be used for a wide class of two-scale linear partial differential operators. Let $\mathcal{V}$ and $\mathcal{W}$ be two Hilbert spaces for functions of y in the cell domain $Y \subset \mathbb{R}^d$ and $\mathcal{V}'$ and $\mathcal{W}'$ be their respective dual spaces. Let f be a map in $\mathcal{W}'$. For each x in the macroscopic domain $\Omega \subset \mathbb{R}^d$, we consider the problem of a linear PDE in y: Find $v \in \mathcal{V}$ such that

$$\mathcal{L}_y(x) v(x, y) = f(y),$$

and integrating we obtain the corresponding weak variational form

$$\mathcal{A}_y(x)(v(x,\cdot),\phi) = (f,\phi) \tag{10}$$

for $\phi \in \mathcal{W}$. Here, $\mathcal{A}_y(x)(\cdot,\cdot)$ is the bilinear form corresponding to the linear partial differential operator $\mathcal{L}_y(x)$ and $(\cdot,\cdot)$ denotes the duality pairing $(\cdot,\cdot)_{\mathcal{W}',\mathcal{W}}$.

Remark. Note here that for the Stokes cell equations, $v(x,y)$ will have components related to velocity and pressure, more precisely, $v(x,y) = (w(x,y),\pi(x,y))$ given by (7) (in the current slowly varying configuration). In addition, the spaces we will need are the same for both the solution and the test spaces $\mathcal{V} = \mathcal{W}$, and hence $\mathcal{V}' = \mathcal{W}'$. We will be more specific about the spaces in section 4. Finally, the domain Y below plays the role of the cell $Y_{\mathcal{F}}$ in our Stokes problem.

We make a general outline of the algorithm.

Step 1: Build nested FE spaces. Fixing the macropoint $x \in \Omega$, we wish to find an approximation $v(x,\cdot) \in \mathcal{V}$, satisfying (10), using a Galerkin FEM. To this end, we build a nested collection of FE spaces for the problem. We denote the nested solution spaces as $\mathcal{V}_0 \subset \mathcal{V}_1 \subset \cdots \subset \mathcal{V}_L \subset \mathcal{V}$ and the trial spaces as $\mathcal{W}_0 \subset \mathcal{W}_1 \subset \cdots \subset \mathcal{W}_L \subset \mathcal{W}$ for L some fixed positive integer. We construct them so that the error between the correct solution $v(x,\cdot) \in \mathcal{V}$ and the Galerkin FE approximation $\bar{v}(x,\cdot)$ decreases in a structured way. More precisely, for $\phi \in \mathcal{W}_{L-i}$, we solve for $\bar{v}(x,\cdot) \in \mathcal{V}_{L-i}$

$$\mathcal{A}_y(x)(\bar{v}(x,\cdot),\phi) = (f,\phi), \tag{11}$$

where $\bar{v}(x,\cdot)$ satisfies the error condition

$$\|v(x,\cdot) - \bar{v}(x,\cdot)\|_{\mathcal{V}} = \inf_{\psi \in \mathcal{V}_{L-i}} \|v(x,\cdot) - \psi\|_{\mathcal{V}} \le C\kappa^i h \|v(x,\cdot)\|_{\mathcal{U}}. \tag{12}$$

Here, h is the error in the finest approximation spaces $(\mathcal{V}_L, \mathcal{W}_L)$ and κ is the FE coarsening factor. The space $\mathcal{U}$ is the regularity for the solution, standard in FEM error expression; cf. [4]. Note that we are clearly limited in the amount of coarsening of our FE approximation spaces. That is, the coarsest error $\kappa^L h$ must still be able to resolve the scales on the cell domain for it to be a meaningful approximation.

Remark. This coarsening may be accomplished by coarsening the mesh or, conversely, refining. In the numerical example in this work, we start with the lowest level space $\mathcal{V}_0$ and refine the mesh to build the collection of FEM spaces. This process can be seen in Figure 5 in section 5.

Step 2: Build hierarchy of macrogrids. To choose judiciously at which macro–grid points we will solve with high accuracy and which we will solve with lower accuracy correction terms, we must build a hierarchy of macro–grid points. First, we must build a nested macrogrid for Ω, denoted as

$$\mathcal{T}_0 \subset \mathcal{T}_1 \subset \cdots \subset \mathcal{T}_L \subset \Omega.$$

We construct this grid inductively as follows. Suppose we have an initial grid $\mathcal{T}_0$ with grid spacing H. Grid spacing is where the distance between neighboring nodes is at most H. Proceeding inductively, we construct the refinement of $\mathcal{T}_{i-1}$, namely $\mathcal{T}_i$, with grid spacing $H\kappa^{-i}$. Note that the refinement is inversely of the same order as the FE coarsening factor of the error expression (12) for the nested FE spaces.

We then define the dense hierarchy of macrogrids $\{S_0, S_1, \ldots, S_L\}$ inductively as $S_0 = \mathcal{T}_0$, $S_1 = \mathcal{T}_1 \backslash S_0$, and in general

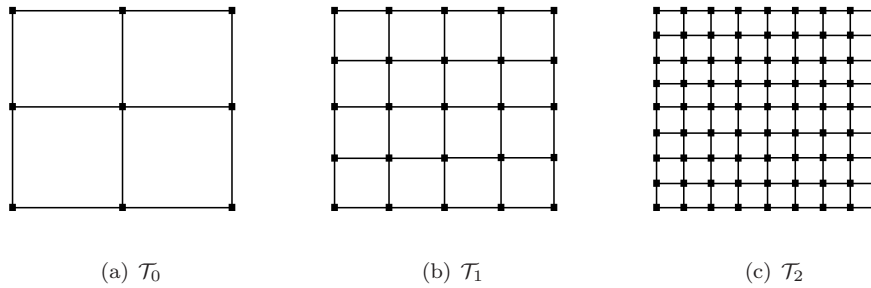$$S_i = \mathcal{T}_i \backslash \left(\bigcup_{k<i} S_k \right).$$

(a) $\mathcal{T}_0$ (b) $\mathcal{T}_1$ (c) $\mathcal{T}_2$

FIG. 2. *3-level nested macrogrids.*
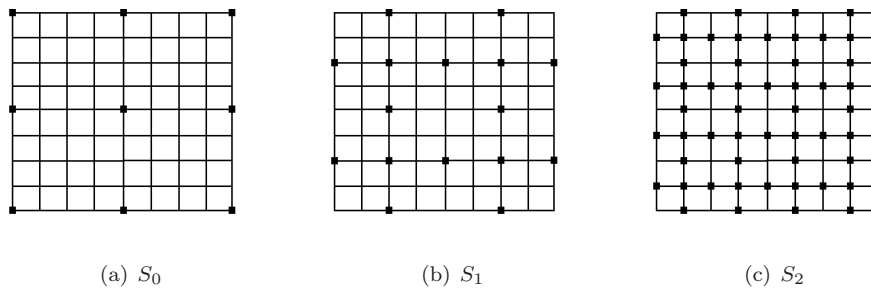

(a) S_0 (b) S_1 (c) S_2

FIG. 3. *3-level hierarchy of macrogrids.*

We refer to the coarsest grid S_0 as the anchor points. We require that the hierarchy of macrogrids be dense. That is, we require that for each point $x \in S_i$, there exists at least one point $x' \in \bigcup_{k<i} S_k$ such that $\mathrm{dist}\,(x, x') < O(H\kappa^{-i})$. An example of a 3-level nested and corresponding hierarchy of macrogrids $\{(\mathcal{T}_i, \mathcal{S}_i)\}_{i=0}^2$, contained in $\Omega = [0,1]^2$, can be seen in Figures 2 and 3.

Step 3: Calculating the correction term. We now relate the nested FE spaces and the hierarchy of macrogrids in an efficient computational scheme. We begin by solving at the so-called anchor points. At these points, we solve using the standard Galerkin FEM. Let $x \in S_0$, the most sparse macrogrid; then, we solve the corresponding cell problems in the space of highest accuracy. That is, we find $\bar{v}(x, \cdot) \in \mathcal{V}_L$, which satisfies

$$(13) \qquad \mathcal{A}_y\,(x)\,(\bar{v}(x, \cdot), \phi) = (f, \phi) \quad \forall\, \phi \in \mathcal{W}_L.$$

We then proceed inductively: for $i = 1, \dots, L$, let $x \in S_i$, and let $\{x_1, x_2, \dots, x_n\} \in (\bigcup_{k<i} S_k)$ be a collection of points sufficiently close to x. More precisely, the distance between x and $\{x_1, x_2, \dots, x_n\}$ is less than $O\left(H\kappa^{-i}\right)$ for all points in the collection. There exists at least one such point in $(\bigcup_{k<i} S_k)$ since we constructed the hierarchy of grids in a dense way. We denote the ith macro–grid interpolation as

$$(14) \qquad I_i^x(v) = \sum_{j=1}^n c_j v(x_j, \cdot),$$

where the constant weights c_j determine the interpolation procedure. We also require $\sum_{j=1}^{n} c_j = 1$. Let $I_i^x(\bar{v}) = \sum_{j=1}^{n} c_j \bar{v}(x_j, \cdot)$ denote the macro–grid interpolation of Galerkin approximations. Recall that we assume we have already computed $\{\bar{v}(x_j, \cdot)\}_{j=1}^{n}$ inductively. We solve for the correction term $\bar{v}_c(x, \cdot) \in \mathcal{V}_{L-i}$ so that

$$\mathcal{A}_y(x)(\bar{v}_c(x, \cdot), \phi) = (f, \phi) - \mathcal{A}_y(x)(I_i^x(\bar{v}), \phi)$$

for all $\phi \in \mathcal{W}_{L-i}$. Note that the right-hand-side term is known data from the previous finer accuracy solves at macro–grid points in $(\bigcup_{k<i} S_k)$. We solve for the correction term in a set of FE spaces $(\mathcal{V}_{L-i}, \mathcal{W}_{L-i})$ with coarser accuracy. Using both the correction term and the macro–grid interpolation term, let

(15) $$\bar{v}(x, \cdot) = \bar{v}_c(x, \cdot) + I_i^x(\bar{v})$$

be an approximation for $v(x, \cdot)$. We will show in section 3 that the approximation (15) for $v(x, \cdot)$ is of the same order of accuracy as if we solved in the standard way via (13) using the finest FE spaces $(\mathcal{V}_L, \mathcal{W}_L)$, at a reduced computational cost.

The simplest macro–grid interpolation scheme is that of a single point, $I_i^x(v) = v(x_1, \cdot)$, for some $x_1 \in (\bigcup_{k<i} S_k) \bigcap B_{H\kappa^{-i}}(x)$. Here, $B_{H\kappa^{-i}}(x)$ is an open ball in Ω centered at x with radius $H\kappa^{-i}$. Another simple scheme is the two-point scheme. For some $x_1, x_2 \in (\bigcup_{k<i} S_k) \bigcap B_{H\kappa^{-i}}(x)$, we write $I_i^x(v) = \frac{1}{2}(v(x_1, \cdot) + v(x_2, \cdot))$, and so on.

Remark. The relationship between the error coarsening factor κ of the nested FE spaces and the refinement of the hierarchy of macrogrids is critical. The coarser the FE spaces, the closer the macro–grid points must be when calculating the correction term. Conversely, for very fine resolution FE solves, we use a sparser macrogrid. With this in mind, we see that Steps 1 and 2 can be interchanged in order.

3. Abstract formulation. In this section, we enumerate the assumptions and conditions required to guarantee that our efficient multiscale algorithm will yield the same accuracy as the full solve. These assumptions on the variational form (10) are physically reasonable and easily verifiable. To illustrate the main of ideas of the proof of the error estimate, we proceed to build a nested collection of FE spaces and a corresponding hierarchy of macrogrids for $\Omega = [0, 1]^2$. We proceed as outlined in section 2.2.

We show in Theorem 3.1, without loss of generality, that we are able to obtain the same order of accuracy as the full solve. For large domains with large variation in microstructure over the domain, we must resolve the local scales at many macroscopic points. We must solve many cell problems, each of which can be computationally expensive. Indeed, if we have $O(M)$ cell problems and in each cell we have $O(N)$ unknowns, then the total number of degrees of freedom for the full solve is $O(MN)$. Comparatively, the hierarchical solve will be that of one single set of cell equations or $O(N)$ degrees of freedom, a significant reduction. The computational complexity is summarized in Theorem 3.2.

3.1. Assumptions on the operator. To ensure that our algorithm will give us the proper rate of convergence we must make a few abstract assumptions on the variational form (10). The first one is a standard assumption. These conditions are the boundedness, the so-called inf-sup, and the nondegeneracy conditions; cf. [11]. They guarantee the existence, uniqueness, and a priori bounds for the solution.

Assumption 3.1. There are positive constants α and β, independent of the nested FE spaces, so that for all $x \in \Omega$

(16a)
$$\sup_{v \in \mathcal{V}, w \in \mathcal{W}} \frac{|\mathcal{A}_y(x)(v, w)|}{\|v\|_\mathcal{V} \|w\|_\mathcal{W}} \leq \alpha < \infty,$$

(16b)
$$\inf_{0 \neq v} \sup_{0 \neq w} \frac{|\mathcal{A}_y(x)(v, w)|}{\|v\|_\mathcal{V} \|w\|_\mathcal{W}} \geq \beta > 0,$$

(16c)
$$\forall 0 \neq w \in \mathcal{W}: \sup_{v \in \mathcal{V}} |\mathcal{A}_y(x)(v, w)| > 0.$$

With Assumption 3.1, problem (10) has a unique solution v that satisfies the a priori bounds

$$\|v\|_\mathcal{V} \leq \frac{1}{\beta} \|f\|_{\mathcal{W}'}.$$

To utilize information from solutions at other nearby macro–grid points, we must have some measure of how much the variational form may change from macropoint to macropoint in Ω. The following assumption that the variational form must be Lipschitz in x allows us to quantify this idea.

Assumption 3.2. There exists a constant γ, independent of the nested FE spaces, so that for all $x, x' \in \Omega$

$$|(\mathcal{A}_y(x) - \mathcal{A}_y(x'))(v, w)| \leq \gamma |x - x'| \|v\|_\mathcal{V} \|w\|_\mathcal{W}.$$

To ensure accuracy of the finite element approximations we must assume regularity of the true solution and existence of a regularity space $\mathcal{U}$. For the canonical example, the Laplacian operator $-\Delta$ using a linear Lagrange FE we have $\mathcal{V} = H^1(Y)$ and $\mathcal{U} = H^2(Y)$ [11]. We also have specific requirements on the FE error. We summarize this in an assumption.

Assumption 3.3. There is a regularity space $\mathcal{U}$, containing $\mathcal{V}$, and a nested sequence of finite element spaces $\mathcal{V}_0 \subset \mathcal{V}_1 \subset \cdots \subset \mathcal{V}_L \subset \mathcal{V}$ so that for all v in $\mathcal{U}$

(17)
$$\inf_{\psi \in \mathcal{V}_{L-i}} \|v - \psi\|_\mathcal{V} \leq \theta \left(1 + \frac{\alpha}{\beta}\right) \kappa^i h \|v\|_\mathcal{U},$$

where the constant θ depends only on the spaces $\mathcal{U}, \mathcal{V}$ and the domain Ω. The constants α and β are as in Assumption 3.1. Here, h is the order of accuracy for the finest space $\mathcal{V}_L$ and κ is the FE coarsening factor.

For the purpose of formulating the finite element approximations of (10), we assume that the boundedness, inf-sup, and nondegeneracy conditions hold for the discrete problem, and the constants are independent of the nested FE spaces. This may be guaranteed by choosing proper stable FE spaces. For example, for Stokes equations we can use $\mathbb{P}_k/\mathbb{P}_{k-1}$, $k \geq 2$, Taylor–Hood elements; cf. [11]. In section 5, we use the stable element $\mathbb{P}_2/\mathbb{P}_0$ in the implementation of our algorithm. We summarize this requirement in an assumption.

Assumption 3.4. There is a nested sequence of finite element spaces $\mathcal{W}_0 \subset \mathcal{W}_1 \subset$

$\cdots \subset \mathcal{W}_L \subset \mathcal{W}$ so that

$$(18a) \qquad \sup_{v \in \mathcal{V}_i, w \in \mathcal{W}_i} \frac{|\mathcal{A}_y(x)(v,w)|}{\|v\|_{\mathcal{V}}\|w\|_{\mathcal{W}}} \leq \alpha < \infty,$$

$$(18b) \qquad \inf_{0 \neq \mathcal{V}_i} \sup_{0 \neq \mathcal{W}_i} \frac{|\mathcal{A}_y(x)(v,w)|}{\|v\|_{\mathcal{V}}\|w\|_{\mathcal{W}}} \geq \beta > 0,$$

$$(18c) \qquad \forall\, 0 \neq w \in \mathcal{W}_i : \ \sup_{v \in \mathcal{V}_i} |\mathcal{A}_y(x)(v,w)| > 0$$

for $i = 0, 1, \ldots, L$, and the spaces $\mathcal{V}_0 \subset \mathcal{V}_1 \subset \cdots \subset \mathcal{V}_L \subset \mathcal{V}$ are as in Assumption 3.3. The constants α and β are the same as in Assumption 3.2.

To ensure that our macro–grid interpolation (14) is close to the solution of (10), we assume the following regularity condition with respect to the macrovariable x. This assumption assumes a slow changing microstructure. With this regularity we can show by a simple Taylor expansion argument the following inequality.

Assumption 3.5. The solution v of the problem (10) is in $C^1(\bar{\Omega})$ as a map from $v(x, \cdot) : \Omega \to \mathcal{U}$. Let $I_i^x(v)$ be the interpolating operator in (14); then we have

$$\|v(x, \cdot) - I_i^x(v)\|_{\mathcal{U}} \leq N \max_{j=1}^{n} (d(x, x_j))$$

for some $N > 0$, independent of the nested FE spaces, and d is the standard Euclidean metric.

Remark. The above assumption relies heavily on the smoothness of our mapping. We have not provided a proof of this result, and it will be taken as an assumption throughout this work. However, for smooth mappings (i.e., slowly varying geometries) one expects this assumption to be valid. This is a subject of great interest and future work.

3.2. Proof of the main theorem for the two-dimensional macrogrid. In this section we construct a rectangular hierarchy of macrogrids and corresponding nested FE spaces that satisfy the assumptions of the algorithm outlined in section 2.2, where $\Omega = [0,1]^2$ and $Y = [0,1]^2$. We prove that by using the assumptions on the variational form (10) outlined in section 3.1, we obtain the same order of convergence as the full solve. The proof generalized to $\Omega \subset \mathbb{R}^d$ and $Y \subset \mathbb{R}^d$ can be achieved in a similar manner. We proceed in this way with the intent of elucidating elements of the proof without loss of generality.

We begin by outlining the FE spaces needed in the proof. Here, the explicit representation of the FE spaces is not so important, but the proper error bounds are crucial. Let $(\mathcal{V}_i, \mathcal{W}_i)_{i=1}^{L}$ be FE spaces over Y satisfying the assumptions in section 3.1. In this case, $\mathcal{V}_0 = \mathcal{W}_0 = \emptyset$ for simplicity of notation of indices, as it is convenient here to reindex. Furthermore, let $v_i \in \mathcal{V}_i$ be such that

$$(19) \qquad \mathcal{A}_y(x)(v_i(x, \cdot), \phi) = (f, \phi) \quad \forall \phi \in \mathcal{W}_i.$$

From Assumption 3.4, this problem has a unique solution $v_i \in \mathcal{V}_i$. In addition, from Assumption 3.3 we have the error estimate

$$\|v(x, \cdot) - v_i(x, \cdot)\|_{\mathcal{V}} = \left(1 + \frac{\alpha}{\beta}\right) \inf_{\phi \in \mathcal{V}_i} \|v - \phi\|_{\mathcal{V}} \leq \theta \left(1 + \frac{\alpha}{\beta}\right) 2^{-i} \|v\|_{\mathcal{U}}.$$

Here, we have that $h = 2^{-L}$ is the accuracy of the finest space $\mathcal{V}_L$ and $\kappa = 2$ is the FE coarsening factor. As v is a continuous map from Ω to $\mathcal{U}$, $\|v(x, \cdot)\|_{\mathcal{U}}$ is bounded

uniformly for all $x \in \Omega$. Therefore, there is a constant M such that

$$(20) \qquad \|v(x, \cdot) - v_i(x, \cdot)\|_{\mathcal{V}} \leq M 2^{-i}$$

for all $i = 1, \ldots, L$, and all $x \in \Omega$.

For simplicity, in the following presentation, we assume that the macroscopic domain Ω is the closed cube $[0,1]^2 \subset \mathbb{R}^2$. In the interval $[0,1]$, let T_0 be the set $\{0, 1/2, 1\}$ and, for $k \geq 1$, let T_k be the set $\{(2j-1)2^{-(k+1)}, j = 1, 2, 3, \ldots, 2^k + 1\}$. We define the set $S_i \subset \Omega$ as

$$S_i = \{x = (x_1, x_2), \ x_k \in T_{i_k} : \ \max\{i_1, i_2\} = i\},$$

and we let $S = \cup_{i=0}^{L-1} S_i$, where $S_L = \emptyset$ due to reindexing. The first few of both nested and hierarchical macrogrids can be seen in Figures 2 and 3. Clearly, this hierarchy of macrogrids satisfies the grid spacing and density requirements. We will show with the above hierarchy of macrogrids $\{S_i\}_{i=0}^{L-1}$ and nested FE spaces $(\mathcal{V}_i, \mathcal{W}_i)_{i=1}^{L}$ that the algorithm outlined in section 2.2 yields accuracy equivalent to that when using finest FE space $\mathcal{V}_L$ for all points S.

We begin by establishing standard Galerkin approximation at the anchor points as a base step to our induction. For each point $x \in S_0$, we consider the Galerkin approximation (19) using the finest FE spaces $(\mathcal{V}_L, \mathcal{W}_L)$ and we find the solution $\bar{v}(x, \cdot) \in \mathcal{V}_L$ such that

$$\|v(x, \cdot) - \bar{v}(x, \cdot)\|_{\mathcal{V}} \leq M 2^{-L}.$$

We then find the Galerkin approximations for (10) at other points $x \in S$ inductively as follows. Consider a point $x = (x_1, x_2)$ in S_i, i.e., $x_1 \in T_{i_1}$ and $x_2 \in T_{i_2}$, $\max\{i_1, i_2\} = i$. Let $x_1 = (2j_1 - 1)2^{-i_1}$ and $x_2 = (2j_2 - 1)2^{-i_2}$. Let

$$x' = (2(j_1 - 1)2^{-i_1}, (2j_2 - 1)2^{-i_2}) \ \text{ if } \ i_1 > i_2,$$
$$x' = ((2j_1 - 1)2^{-i_1}, 2(j_2 - 1)2^{-i_2}) \ \text{ if } \ i_1 < i_2,$$
$$x' = (2(j_1 - 1)2^{-i_1}, 2(j_2 - 1)2^{-i_2}) \ \text{ if } \ i_1 = i_2.$$

It is clear that $x' \in S_{i'}$, where $i' < i$, and in any case, $d(x, x') < \sqrt{2} \cdot 2^{-i}$. Assume that a Galerkin approximation $\bar{v}(x', \cdot) \in \mathcal{V}_{L-i'}$ has been computed for $v(x', \cdot)$. We consider the following problem: Find the correction term, $\bar{v}_c(x, \cdot) \in \mathcal{V}_{L-i}$, so that

$$(21) \qquad \mathcal{A}_y(x)(\bar{v}_c(x, \cdot), \phi) = (f, \phi) - \mathcal{A}_y(x)(\bar{v}(x', \cdot), \phi)$$

for all $\phi \in \mathcal{W}_{L-i}$. Let the approximation for $v(x, \cdot)$ be given by

$$\bar{v}(x, \cdot) = \bar{v}_c(x, \cdot) + \bar{v}(x', \cdot).$$

Note here that we use the single point interpolation $I_i^x(v) = v(x', \cdot)$ as in (14). We have the following proposition for $\bar{v}(x, \cdot)$ constructed in such a way.

PROPOSITION 3.1. *There is a positive constant c_i which depends only on the operator $\mathcal{L}_y$ and i so that*

$$(22) \qquad \|v(x, \cdot) - \bar{v}(x, \cdot)\|_{\mathcal{V}} \leq c_i 2^{-L}.$$

Proof. We prove (22) by induction. The conclusion obviously holds for $i = 0$. We assume that the conclusions hold for all $l < i$. Let $x \in S_i$ and $x' \in S_{i'}$, for $i' < i$, be as above, and let the continuous correction term be given by

$$v_c(x, y) = v(x, y) - v(x', y).$$

Sufficient smoothness for $v(x, \cdot) : \Omega \to \mathcal{U}$ is guaranteed from Assumption 3.5, and, using $d(x, x') \leq \sqrt{2} \cdot 2^{-i}$, we have the estimate

$$(23) \qquad \|v_c(x, \cdot)\|_{\mathcal{U}} \leq N d(x, x') \leq N 2^{-i},$$

where we absorb the factor $\sqrt{2}$ into N. From the variational formulation on the continuous level we have

$$\mathcal{A}_y(x)(v_c(x, \cdot), \phi) = (f, \phi) - \mathcal{A}_y(x)(v(x', \cdot), \phi)$$

for all $\phi \in \mathcal{W}$. Recall that we have solved

$$\mathcal{A}_y(x')(v(x', \cdot), \phi) = (f, \phi);$$

from here we deduce that

$$\mathcal{A}_y(x)(v_c(x, \cdot), \phi) = -(\mathcal{A}_y(x) - \mathcal{A}_y(x'))(v(x', \cdot), \phi).$$

Let $\bar{\bar{v}}_c(x, \cdot) \in \mathcal{V}_{L-i}$ be such that

$$(24) \qquad \mathcal{A}_y(x)(\bar{\bar{v}}_c(x, \cdot), \phi) = -(\mathcal{A}_y(x) - \mathcal{A}_y(x'))(v(x', \cdot), \phi) \quad \forall \, \phi \in \mathcal{W}_{L-i}.$$

From Assumption 3.4 and Cea's lemma [4], we obtain

$$\|v_c(x, \cdot) - \bar{\bar{v}}_c(x, \cdot)\|_{\mathcal{V}} = \left(1 + \frac{\alpha}{\beta}\right) \inf_{\phi \in \mathcal{V}_{L-i}} \|v_c - \phi\|_{\mathcal{V}}.$$

From (17) and (23), we deduce that

$$\|v_c(x, \cdot) - \bar{\bar{v}}_c(x, \cdot)\|_{\mathcal{V}} \leq \theta \left(1 + \frac{\alpha}{\beta}\right) 2^{i-L}(N 2^{-i}) \leq \theta \left(1 + \frac{\alpha}{\beta}\right) N 2^{-L}.$$

Since $x' \in S_{i'}$, where $i' < i$, then $\mathcal{V}_{L-i} \subset \mathcal{V}_{L-i'}$. Recall that we have previously computed $\bar{v}(x', \cdot) \in \mathcal{V}_{L-i'}$, an FE space with higher accuracy. Therefore, $\bar{v}(x', \cdot)$ will satisfy the variational form (19) over nested spaces with lower accuracy. More precisely, we will have

$$(25) \qquad \mathcal{A}_y(x')(\bar{v}(x', \cdot), \phi) = (f, \phi) \quad \forall \, \phi \in \mathcal{W}_{L-i}.$$

From (21) and (25), we deduce that

$$(26) \qquad \mathcal{A}_y(x)(\bar{v}_c(x, \cdot), \phi) = -(\mathcal{A}_y(x) - \mathcal{A}_y(x'))(\bar{v}(x', \cdot), \phi) \quad \forall \, \phi \in \mathcal{W}_{L-i}.$$

Therefore, from Assumption 3.4 and using (24) and (26),

$$\|\bar{\bar{v}}_c(x, \cdot) - \bar{v}_c(x, \cdot)\|_{\mathcal{V}} \leq \frac{1}{\beta} \|(\mathcal{A}_y(x) - \mathcal{A}_y(x'))(v(x', \cdot) - \bar{v}(x', \cdot))\|_{\mathcal{W}'}.$$

Finally, using the Lipschitz assumption (Assumption 3.2), we obtain

$$\begin{aligned}
\|(\mathcal{A}_y(x) - \mathcal{A}_y(x'))(v(x', \cdot) - \bar{v}(x', \cdot))\|_{\mathcal{W}'} &\leq \gamma |x - x'| \|v(x', \cdot) - \bar{v}(x', \cdot)\|_{\mathcal{V}} \\
&\leq \gamma (\sqrt{2} \cdot 2^{-i})(c_i 2^{-L}) \leq \sqrt{2} c_i \gamma 2^{-L-i}.
\end{aligned}$$

Therefore,

$$\|\bar{\bar{v}}_c(x,\cdot) - \bar{v}_c(x,\cdot)\|_\mathcal{V} \le \frac{\sqrt{2}}{\beta} c_i \gamma 2^{-L-i}.$$

Thus, putting all the estimates together we obtain

$$\|v(x,\cdot) - \bar{v}(x,\cdot)\|_\mathcal{V} \le \|v_c(x,\cdot) - \bar{v}_c(x,\cdot)\|_\mathcal{V} + \|v(x',\cdot) - \bar{v}(x',\cdot)\|_\mathcal{V} \le c_{i+1} 2^{-L},$$

where

$$(27) \qquad c_{i+1} = c_i + \frac{\sqrt{2}}{\beta} c_i \gamma 2^{-i} + \left(1 + \frac{\alpha}{\beta}\right) \theta N. \qquad \square$$

We are now in the position to prove our main result.

THEOREM 3.1. *Let the assumptions of Proposition* 3.1 *hold. Furthermore, assume we have constructed* $\bar{v}(x,\cdot)$ *as above for* $x \in S_i$. *Then, for a sufficiently large constant* c_* *which depends only on the operator* $\mathcal{L}_y$, *we have the estimate*

$$\|v(x,\cdot) - \bar{v}(x,\cdot)\|_\mathcal{V} \le c_*(i+1)2^{-L}.$$

Proof. We choose a constant $\bar{i}$ independent of L such that $i2^{-i} < \beta/(2\sqrt{2}\gamma)$ for $i > \bar{i}$. Let

$$c_* = \max\left\{\max_{0 \le i \le \bar{i}} \left\{\frac{c_i}{i}\right\}, 2\left(1 + \frac{\alpha}{\beta}\right)\theta N\right\},$$

where c_i is given by (27). We prove that

$$(28) \qquad \|v(x,\cdot) - \bar{v}(x,\cdot)\|_\mathcal{V} \le c_*(i+1)2^{-L}$$

by induction. This obviously holds for all $i \le \bar{i}$. We assume that the conclusions hold for all i. From (27), we deduce that

$$c_{i+1} \le ic_* + \frac{\sqrt{2}\gamma}{\beta}\frac{\beta}{2\sqrt{2}\gamma}c_* + \frac{c_*}{2} \le (i+1)c_*.$$

The theorem is proved. $\square$

We also state a theorem on the computational complexity of our algorithm for such a hierarchy of macrogrids and FE spaces given in this section.

THEOREM 3.2. *Suppose that we solve* (10) *for* x *in* $S_0, S_1, \ldots, S_L$ *and that the total number of degrees of freedom is* $\mathcal{O}(L2^{2L})$ *for the hierarchical solve. Comparatively, the number of degrees of freedom in the full solve is* $\mathcal{O}((2^{2L})^2)$.

Proof. First note that the dimension of $\mathcal{V}_{L-i}$ is $\mathcal{O}(2^{2(L-i)})$ and that the number of points in S_i is $\mathcal{O}(2^{2i})$. Therefore, the total number of degrees of freedom when solving (10) for all points in S_i is $\mathcal{O}(2^{2i})\mathcal{O}(2^{2L-2i}) = \mathcal{O}(2^{2L})$. Thus, the total number of degrees of freedom used when solving (10) for all points in $S_0, S_1, \ldots, S_L$ is $\mathcal{O}(L2^{2L})$. $\square$

Remark. It is important to note the connection between the number of macro–grid points and degrees of freedom for local problems. To obtain the above optimal computational result, the relationship between the two is critical. If one wanted to increase the size of the macroscopic domain, more macro–grid points would increase. For example, if we were to square the number of points $S_i = O(2^{2i}) \rightarrow S_i = O(2^{4i})$, we would make a corresponding change in the accuracy of the FE spaces to obtain the above result.

4. Application to the Stokes equations. In this section, we apply the algorithm and methodology outlined in sections 2.2 and 3 to the modified Stokes equations in the periodic domain. In section 2.1, we gave a brief overview of homogenization of the Stokes equations in slowly varying domains. Here, we use the ALE formulation of the Stokes equations; cf. [12, 13]. We will briefly formulate this reformulation in the periodic domain and will then apply the two-scale asymptotic expansion [20] to the modified equations. This will allow for easy application of our efficient algorithm. The details for the derivation of the ALE formulation and the application of two-scale expansion can be found in the appendix. We obtain auxiliary cell equations and hence the homogenized equations in the periodic ALE.

With the intention of developing a proper nested collection of FE spaces, we then introduce appropriate Sobolev spaces for the solutions. Then, the variational formulation of the cell equations is presented. We make basic assumptions on the smoothness properties of the mapping $\widetilde{\mathbf{x}}_\varepsilon$ and the geometry of the cell equations. With these assumptions we verify that the conditions on the operator outlined in section 3.1 are satisfied. Hence, given a hierarchy of macrogrids and the corresponding nested collection of FE spaces as outlined in section 2.2, satisfying the assumptions in 3.1, we are able to obtain the error estimate given by Theorem 3.1.

4.1. Homogenization of Stokes equations in the ALE formulation. In the slowly varying domains, there is variation of the cell geometry from RVE to RVE. When we reformulate the Stokes equations to the periodic domain, we encode this information into the tensor coefficients of the modified equations. We begin by reformulating the Stokes equations.

Recall that the fine-scale Stokes equations (2) are represented in the slowly varying fluid domain $\widetilde{\mathcal{F}_\varepsilon} = \widetilde{\mathbf{x}}_\varepsilon(\mathcal{F}_\varepsilon)$. Let $\mathcal{P}_\varepsilon \subset \mathcal{F}_\varepsilon$ be some open subset of the periodic fluid domain, and thus $\widetilde{\mathbf{x}}_\varepsilon(\mathcal{P}_\varepsilon) = \widetilde{\mathcal{P}}_\varepsilon$. We rewrite the Stokes equations in integral form after the application of the divergence theorem as

$$(29a) \qquad \int_{\partial\widetilde{\mathcal{P}}_\varepsilon} (-\widetilde{p}_\varepsilon(\tilde{x})\mathbf{I} + \mu\nabla_{\tilde{x}}\widetilde{v}_\varepsilon(\tilde{x})) \cdot \widetilde{n}(\tilde{x})d\tilde{x} = \int_{\widetilde{\mathcal{P}}_\varepsilon} \widetilde{f}(\tilde{x})d\tilde{x},$$

$$(29b) \qquad \int_{\partial\widetilde{\mathcal{P}}_\varepsilon} \widetilde{v}_\varepsilon(\tilde{x}) \cdot \widetilde{n}(\tilde{x})d\tilde{x} = 0.$$

We make the change of variables $\tilde{x} \to \tilde{x}(x)$ and map back to the initial periodic fluid domain. If $\widetilde{\phi}(\tilde{x})$ is a physical quantity in the deformed (slowly varying) domain, then denote the pullback to the periodic domain $\phi(x) := \widetilde{\phi}(\tilde{x}(x))$. We need to define a few tensors. Let the mapping gradient and Jacobian be defined as

$$\mathbf{F}_\varepsilon(x) = \nabla_x\widetilde{\mathbf{x}}_\varepsilon(x), \qquad J_\varepsilon(x) = \det(\nabla_x\widetilde{\mathbf{x}}_\varepsilon(x))$$

and the related tensors as

$$\mathbf{G}_\varepsilon(x) = \det(\mathbf{F}_\varepsilon(x))\mathbf{F}_\varepsilon(x)^{-T}, \qquad \mathbf{H}_\varepsilon(x) = \mathbf{F}_\varepsilon^{-1}(x)\mathbf{G}_\varepsilon(x).$$

We assume that the mapping is nondegenerate; that is, there exists a $c > 0$ such that $J_\varepsilon(x) > c > 0$ for all $x \in \Omega$. Hence, $\mathbf{F}_\varepsilon(x)$ and related tensors will be invertible for all points in the domain. Note that in this coordinate transformation, gradients are transformed as

$$\nabla_{\tilde{x}}\widetilde{v}_\varepsilon(\tilde{x}) = \nabla_x v_\varepsilon(x)\mathbf{F}_\varepsilon^{-1}(x).$$

Let the surface normal on $\partial\widetilde{\mathcal{P}}_\varepsilon$ be $\widetilde{n}$ and the surface normal on $\partial\mathcal{P}_\varepsilon$ be n. The surface normals and volume elements transform as

$$\widetilde{n}(\widetilde{x}) = \mathbf{F}_\varepsilon^{-T}(x)n(x), \qquad d\widetilde{x} = J_\varepsilon(x)dx.$$

Using these transformations, we represent (29) in the periodic domain as

$$\int_{\partial\mathcal{P}_\varepsilon} (-p_\epsilon(x)\mathbf{G}_\varepsilon(x) + \mu\nabla_x v_\varepsilon(x)\mathbf{H}_\varepsilon(x)) \cdot n(x)dx = \int_{\mathcal{P}_\varepsilon} f(x)J_\varepsilon(x)dx,$$

$$\int_{\partial\mathcal{P}_\varepsilon} v_\varepsilon(x) \cdot \mathbf{G}_\varepsilon(x) \cdot n dx = 0.$$

This is true for any $\mathcal{P}_\varepsilon \subset \mathcal{F}_\varepsilon$. We move to the divergence form of these equations, and we obtain the modified Stokes equations in the periodic domain $\mathcal{F}_\varepsilon$:

$$-\text{div}_x\left(p_\varepsilon(x)\mathbf{G}_\varepsilon(x)\right) + \mu\text{div}_x(\nabla_x v_\varepsilon(x)\mathbf{H}_\varepsilon(x)) = f(x)J_\varepsilon(x) \text{ in } \mathcal{F}_\varepsilon, \tag{30a}$$

$$\text{div}_x(\mathbf{G}_\varepsilon^T(x)v_\varepsilon) = 0 \text{ in } \mathcal{F}_\varepsilon, \tag{30b}$$

and we assume the boundary condition that $v_\varepsilon = 0$ on Γ_ε. This is a representation of the fine-scale Stokes operator we denoted earlier by $\mathcal{L}_\varepsilon\left(x, \frac{x}{\varepsilon}\right)$.

Remark. Here we briefly clarify some notation. For scalar quantities ϕ, we write $(\nabla_x\phi)_i = \frac{\partial\phi}{\partial x_i}$ as a column vector. In addition, for vector quantities such as the deformation, we have $(\mathbf{F}_\varepsilon)_{ij} = \frac{\partial\widetilde{\mathbf{x}}_\varepsilon^i}{\partial x_j}$. For matrix-vector multiplication, we use the standard convention of multiplying on the right, summing over the second index of the matrix. Finally, divergence over tensor quantities is summed over the second variable. To illustrate this, we write out (30a) in indicial notation using the Einstein summation convention

$$-\frac{\partial}{\partial x_j}\left((\mathbf{G}_\varepsilon)_{ij}p_\varepsilon\right) + \mu\frac{\partial}{\partial x_j}\left(\frac{\partial v_\varepsilon^i}{\partial x_m}(\mathbf{H}_\varepsilon)_{mj}\right) = f^i J_\varepsilon.$$

For brevity, we will return to using the tensor notation.

We apply the two-scale asymptotic expansions (42)–(46), given in the appendix, and apply them to (30). Gathering terms in ε we obtain the two auxiliary cell equations for $i = 1, \ldots, d$,

$$-\mathbf{G}_0\nabla_y\pi_1^i + \mu\text{div}_y\left(\nabla_y w_1^i\mathbf{H}_0\right) = \mathbf{G}_0 e_i \text{ in } Y_\mathcal{F}, \tag{31a}$$

$$\text{div}_y(\mathbf{G}_0^T w_1^i) = 0 \text{ in } Y_\mathcal{F}, \tag{31b}$$

and for the second cell equation

$$-\mathbf{G}_0\nabla_y\pi_2^i + \mu\text{div}_y\left(\nabla_y w_2^i\mathbf{H}_0\right) = J_0 e_i \text{ in } Y_\mathcal{F}, \tag{32a}$$

$$\text{div}_y(\mathbf{G}_0^T w_2^i) = 0 \text{ in } Y_\mathcal{F}, \tag{32b}$$

where w_j^i and π_j^i are y-periodic, $w_j^i = 0$ on Y_Γ, and $\langle\pi_j^i\rangle_Y = 0$. The two cell equations are a result of the representation (49) for p_1 and v_0. The above partial differential operator is the cell operator denoted by $\mathcal{L}_y(x)$.

From the ε^0 order of the expansion of (30b) and averaging over $Y_\mathcal{F}$ we obtain a representation for the homogenized operator in the periodic domain $\mathcal{L}(x)$. The modified Darcy equation is given by

$$\nabla_x \cdot \left(\mathbf{K}(x)\nabla_x p_0(x) + \bar{f}(x)\right) = 0 \text{ in } \Omega, \tag{33}$$

where

$$\mathbf{K}(x) = \left\langle \mathbf{G}_0^T(x,y) w_1(x,y) \right\rangle_Y \quad \text{and} \quad \bar{f}(x) = \left\langle \mathbf{G}_0^T(x,y) w_2(x,y) \right\rangle_Y f(x).$$

The modified Darcy velocity is given by $\xi = \mathbf{K}(x)\nabla_x p_0(x) + \bar{f}(x)$. We also require the boundary conditions $\xi \cdot \nu = 0$ on $\partial\Omega$, where ν is the unit normal.

4.2. Variational form and verification of algorithm assumptions. In this section, we present definitions of appropriate Sobolev solution spaces. Then, we derive the corresponding variational form for the cell operator in the periodic setting $\mathcal{L}_y(x)$ given by (31) and (32). We show that this variational form will satisfy the abstract assumptions outlined in section 3.1.

We define the following Sobolev spaces. For the pressure related quantities let

$$(L^2_{\int=0}(Y_{\mathcal{F}}))^d = \left\{ \zeta \in (L^2(Y_{\mathcal{F}}))^d : \frac{1}{|Y_{\mathcal{F}}|} \int_{Y_{\mathcal{F}}} \zeta dy = 0 \right\},$$

and for the velocity related quantities let

$$(H^1_{\#,0}(Y_{\mathcal{F}}))^{d\times d} = \{ q \in (H^1(Y_{\mathcal{F}}))^{d\times d} : q = 0 \text{ on } Y_\Gamma \text{ and } q \text{ is } y\text{-periodic} \}.$$

Recall that we have the same solution and test space for our Stokes equations. Indeed, we let

$$(34) \qquad \mathcal{V} = \mathcal{W} = (H^1_{\#,0}(Y_{\mathcal{F}}))^{d\times d} \times (L^2_{\int=0}(Y_{\mathcal{F}}))^d.$$

Remark. For the rest of the paper, when we state the spaces $\mathcal{V}, \mathcal{W}$, we will mean the above cross product of Sobolev spaces with $\mathcal{V} = \mathcal{W}$. Moreover, the spaces $\{\mathcal{V}_l = \mathcal{W}_l\}_{l=0}^L$ will be finite-dimensional FE subspaces of $\mathcal{V}$ given by (34).

Multiplying both sides of (31) and (32) by test functions $(q(y), \zeta(y)) \in \mathcal{V}$ and integrating by parts we obtain a corresponding variational form for each $x \in \Omega$:

$$\mathcal{A}_y(x) \Big((w(x,y), \pi(x,y)), (q(y), \zeta(y)) \Big)$$

$$= \int_{Y_{\mathcal{F}}} \left(\pi(x,y) \cdot \mathrm{div}_y(\mathbf{G}_0^T(x,y) q(y)) - \mu(\nabla_y w(x,y) \mathbf{H}_0(x,y)) : \nabla_y q(y) \right) dy$$

$$(35) \qquad\qquad + \int_{Y_{\mathcal{F}}} \left(\zeta(y) \cdot \mathrm{div}_y(\mathbf{G}_0^T(x,y) w(x,y)) \right) dy.$$

The cell problems (31) and (32) can then be written as the following two variational problems: Find $(w_j(x,y), \pi_j(x,y)) \in \mathcal{V}$, for $j = 1, 2$, such that

$$\mathcal{A}_y(x) \Big((w_1(x,y), \pi_1(x,y)), (q(y), \zeta(y)) \Big) = \int_{Y_{\mathcal{F}}} \mathbf{G}_0(x,y) : q(y) dy,$$

$$\mathcal{A}_y(x) \Big((w_2(x,y), \pi_2(x,y)), (q(y), \zeta(y)) \Big) = \int_{Y_{\mathcal{F}}} J_0(x,y) \mathbf{I} : q(y) dy$$

for all $(q(y), \zeta(y)) \in \mathcal{V}$.

We will now state and prove a lemma that will allow us to use our efficient multiscale finite element algorithm. We verify the necessary abstract assumptions from section 3.1.

LEMMA 4.1. *Assume that Ω and $Y_{\mathcal{F}}$ are sufficiently smooth. Let the mapping be of the form $\widetilde{\mathbf{x}}_\varepsilon(x) = \widetilde{\mathbf{x}}_0(x) + \varepsilon\widetilde{\mathbf{x}}_1(x,y)$ as in (41). Suppose the regularities $\widetilde{\mathbf{x}}_0 \in C^2(\bar{\Omega})$*

and $\widetilde{\mathbf{x}}_1(x, y) \in C^2(\bar{\Omega} \times Y)$. *Assume the mapping is nondegenerate. There exists a $c > 0$ such that for all $x \in \Omega$, $J_\varepsilon(x) = \det(\nabla \widetilde{\mathbf{x}}_\varepsilon(x)) > c > 0$ and $J_0(x, y) = \det(\nabla_x \widetilde{\mathbf{x}}_0(x) + \nabla_y \widetilde{\mathbf{x}}_1(x, y)) > c > 0$. Then, the variational form* (35) *satisfies the abstract assumptions, namely Assumptions* 3.1 *and* 3.2, *required of* $\mathcal{A}_y(x)$.

Proof. First, we verify Assumption 3.1. The boundedness condition (16a) is a simple consequence of the boundedness that the smooth matrix functions J_0, $\mathbf{F}_0$, $\mathbf{G}_0$, and $\mathbf{H}_0$ are of class $C^1(\bar{\Omega} \times Y)$. The nondegeneracy condition (16c) is easily satisfied as in the standard Stokes variational form; cf. [11].

We verify that the variational form satisfies the inf-sup condition (16b). The velocity term is coercive since the tensor $\mathbf{H}_0 = J_0 \mathbf{F}_0^{-1} \mathbf{F}_0^{-T}$ is positive definite. Indeed, $\mathbf{F}_0^{-T}$ and J_0 satisfy the lower bound conditions (44) and (45). Furthermore, the Poincaré inequality is satisfied since $w = 0$ on Y_Γ. Hence, for a positive constant $C > 0$, the following estimate holds:

$$\int_{Y_\mathcal{F}} \nabla_y w \mathbf{H_0} \nabla_y w dy = \int_{Y_\mathcal{F}} \nabla_y w J_0 \mathbf{F}_0^{-1} \mathbf{F}_0^{-T} \nabla_y w dy$$

$$= \int_{Y_\mathcal{F}} |\mathbf{F}_0^{-T} \nabla_y w|^2 J_0 dy > C ||w||_{(H^1(Y_\mathcal{F}))^{d \times d}}^2.$$

The pressure term satisfies the so-called Babuška–Brezzi condition [5]. Indeed, we must show that for all $\pi \in (L^2_{\int=0}(Y_\mathcal{F}))^d$

$$\sup_{w \in (H^1_{\#,0}(Y_\mathcal{F}))^{d \times d}} \frac{\int_{Y_\mathcal{F}} \pi \mathrm{div}_y(\mathbf{G}_0^T w) dy}{||w||_{(H^1(Y_\mathcal{F}))^{d \times d}}} \geq C ||\pi||_{(L^2_{\int=0}(Y_\mathcal{F}))^d}.$$

Let $v = \mathbf{G}_0^T w$; then $||\mathbf{G}_0^{-T} v||_{(H^1_{\#,0}(Y_\mathcal{F}))^{d \times d}} \leq ||\mathbf{G}_0^{-T}||_\infty ||v||_{(H^1_{\#,0}(Y_\mathcal{F}))^{d \times d}}$. Note that the tensor

$$\mathbf{G}_0^{-T}(x, y) = \frac{\nabla_x \widetilde{\mathbf{x}}_0(x) + \nabla_y \widetilde{\mathbf{x}}_1(x, y)}{J_0(x, y)}$$

is bounded since $\widetilde{\mathbf{x}}_0(x) \in C^2(\bar{\Omega})$, $\widetilde{\mathbf{x}}_1(x, y) \in C^2(\bar{\Omega} \times Y)$ and because of the nondegeneracy of $J_0(x, y)$. The standard Stokes operator satisfies the Babuška–Brezzi condition [11]. Indeed, we have

$$\sup_{v \in (H^1_{\#,0}(Y_\mathcal{F}))} \frac{\int_{Y_\mathcal{F}} \pi \mathrm{div}_y(v) dy}{||\mathbf{G}_0^{-T} v||_{(H^1_{\#,0}(Y_\mathcal{F}))^{d \times d}}} \geq \sup_{v \in (H^1_{\#,0}(Y_\mathcal{F}))} C \frac{\int_{Y_\mathcal{F}} \pi \mathrm{div}_y(v) dy}{||v||_{(H^1_{\#,0}(Y_\mathcal{F}))^{d \times d}}} \geq C ||\pi||_{(L^2_{\int=0}(Y_\mathcal{F}))^d}.$$

Therefore, the variational form $\mathcal{A}_y(x)$ satisfies the inf-sup conditions (16b) and we obtain the desired a priori bound on the initial data.

The variational form $\mathcal{A}_y(x)$ is Lipschitz in the sense outlined in Assumption 3.2. Note that $\mathbf{G}_0$ and $\mathbf{H}_0$ are of class $C^1(\bar{\Omega} \times Y)$, $\bar{\Omega} \times Y$ being compact, and hence they are Lipschitz in x and are bounded (the derivatives are also bounded). In addition, note, based on Stokes regularity results (cf. [3, 21]), that (w, π) are bounded in $(H^1(Y_\mathcal{F}))^{d \times d} \times (L^2(Y_\mathcal{F}))^d$. From these facts we are able to derive the following estimates for (31):

$$||w(x, \cdot) - w(x', \cdot)||_{(H^1(Y_\mathcal{F}))^{d \times d}} + ||\pi(x, \cdot) - \pi(x', \cdot)||_{(L^2(Y_\mathcal{F}))^d}$$
$$\leq C \Big(||\mathbf{G}_0^T(x, \cdot) - \mathbf{G}_0^T(x', \cdot)||_{(H^1(Y_\mathcal{F}))} + ||\mathbf{H}_0(x, \cdot) - \mathbf{H}_0(x', \cdot)||_{(H^1(Y_\mathcal{F}))} \Big).$$

From the above a priori bound, the Lipschitz property of the tensors, and the fact that (q, ζ) are functions of y only, we are able to obtain our result. Indeed, we have for $x, x' \in \Omega$

$$|\mathcal{A}_y(x)(w, \pi), (q, \zeta) - \mathcal{A}_y(x')(w', \pi'), (q, \zeta)|q$$

$$\leq CC\left(||\mathbf{G}_0^T(x, \cdot) - \mathbf{G}_0^T(x', \cdot)||_{(H^1(Y_\mathcal{F}))} + ||\mathbf{H}_0(x, \cdot) - \mathbf{H}_0(x', \cdot)||_{(H^1(Y_\mathcal{F}))}\right) \leq C|x - x'|,$$

where C depends on the norms of (w, π) and (q, ζ) and the Lipschitz constants of $\mathbf{G}_0^T$ and $\mathbf{H}_0$. ☐

Remark. Concerning the regularity space $\mathcal{U}$ of Assumption 3.3, we may obtain the desired regularity of the cell problem by assuming appropriate smoothness on the cell geometry, the mapping, and related tensors. We suppose the regularity space $\mathcal{U} = (H^2(Y_\mathcal{F}))^{d \times d} \times (H^1(Y_\mathcal{F}))^d$. For more on regularity issues of Stokes equations we refer the reader to [3, 21].

With Lemma 4.1, and utilizing the proof of Theorem 3.1, we are now in a position to summarize our results in a theorem. We have the following error estimate for our efficient multiscale FEM applied to the modified cell equations (31) and (32).

THEOREM 4.2. *Suppose the assumptions in Lemma* 4.1 *hold. Suppose that* (w, π) *as a map from* Ω *to* $\mathcal{U} = (H^2(Y_\mathcal{F}))^{d \times d} \times (H^1(Y_\mathcal{F}))^d$ *is in* $C^1(\Omega)$ *to satisfy Assumption* 3.5. *Suppose further that the nested sequence of FE spaces* $\{\mathcal{V}_l\}_{l=0}^L$ *satisfies the error bounds, and* inf*-*sup *conditions of Assumption* 3.4. *Let* $\{S_l\}_{l=0}^L$ *be a dense hierarchy of macrogrids having the properties outlined in section* 2.2. *Then, the FE approximate solutions* $(\bar{w}_j(x, \cdot), \bar{\pi}_j(x, \cdot))$ *to* (31) *and* (32), *constructed as in section* 2.2, *satisfy the error estimate*

$$(36) \qquad \|\pi_j(x, \cdot) - \bar{\pi}_j(x, \cdot)\|_{L^2(Y_\mathcal{F})} + \|w_j(x, \cdot) - \bar{w}_j(x, \cdot)\|_{H^1(Y_\mathcal{F})} \leq c_*(l+1)h.$$

Remark. Any pairs of finite element approximating spaces in $\mathcal{V}$, given by (34), that satisfy the inf-sup condition for the Stokes equations will satisfy the inf-sup condition for the operator $\mathcal{A}_y(x)$ in (35). The proof is identical to that presented above in Lemma 4.1. More precisely, elements stable for the standard Stokes equations will be stable for our modified equations. In the numerical examples below, we choose the well-known Taylor–Hood-type $\mathbb{P}_2/\mathbb{P}_0$ elements.

5. Numerical example. In this section, we propose an example for the implementation of the efficient multiscale FEM method. We apply the computational methodology outlined in section 2.2 to the Stokes cell equations $\mathcal{L}_y(x)$ in the ALE formulation as in section 4. We begin by constructing an initial periodic reference domain Ω. Then, we propose a mapping $\widetilde{\mathbf{x}}_\varepsilon$ that is smooth and depends only on the macroscopic slow variable in one direction. This symmetry makes the macrogrid essentially one dimensional. We build a nested sequence of four FE spaces by decreasing mesh size and construct a hierarchy of macrogrids. After averaging, we compute a component of the modified permeability. We do this for a small stretch and a large stretch mapping. Finally, we compare our fine mesh standard solve to our efficient hierarchical solve for both mappings.

5.1. Example problem formulation. Here, we formulate our example domain, mapping, corresponding equations, and variational form. We begin with the description of the periodic domain. Let $\Omega = [0, 1]^2$ be the macroscopic domain, and define the unit cell to be $Y = [0, 1]^2$. The solid part of the cell is given by the square inclusion $Y_\mathcal{S} = [1/4, 3/4]^2$, and hence the fluid domain is given by $Y_\mathcal{F} = Y \backslash Y_\mathcal{S}$. The

interface of the cell Y_Γ is $\partial Y_\mathcal{S}$. Thus, $\mathcal{F}_\varepsilon$ and $\mathcal{S}_\varepsilon$, periodic fluid and solid domains, are given by (1). Since the domain is periodic, we will have a single unit cell $Y = Y_\mathcal{F} \cup Y_\mathcal{S}$.

We suppose the mapping $\widetilde{\mathbf{x}}_\varepsilon : \Omega \to \widetilde{\Omega}_\varepsilon$ to be a stretch in the x_1 direction given by

$$(37) \qquad \widetilde{\mathbf{x}}_\varepsilon(x) = (x_1, x_2) + \alpha(x_1^2, 0),$$

where $x = (x_1, x_2)$ are coordinates in Ω. This map preserves the periodicity in the x_2 direction, but periodicity in the x_1 direction is broken. Fixing x_1 but varying x_2 will yield the same cell solution, making the macrogridding essentially one dimensional. It is important to note that the local cell problems in $y = (y_1, y_2)$ are still two dimensional in Y.

Recall the two-scale representation for $\widetilde{\mathbf{x}}_\varepsilon(x) = \widetilde{\mathbf{x}}_0(x) + \varepsilon\widetilde{\mathbf{x}}_1(x)$ as in (41). We see that $\widetilde{\mathbf{x}}_1 = 0$, as there is no dependence on ε or the fast variable $y = (y_1, y_2)$. Thus, $\widetilde{\mathbf{x}}_\varepsilon(x) = \widetilde{\mathbf{x}}_0(x)$. Calculating the gradient of this mapping we see that

$$\mathbf{F}_0(x_1) = \begin{pmatrix} 1 + 2\alpha x_1 & 0 \\ 0 & 1 \end{pmatrix},$$

and from here we may build the Jacobian and related tensors $J_0(x_1) = \det(\mathbf{F}_0(x_1))$, $\mathbf{G}_0(x_1) = J_0(x_1)\mathbf{F}_0^{-T}(x_1)$, and $\mathbf{H}_0(x_1) = \mathbf{F}_0^{-1}(x_1)\mathbf{G}_0(x_1)$.

To simplify the implementation, we assume that we have no external body force, that is, $f = 0$. If the body force in present, we must solve two cell problems (31) and (32). We wish to find $(w^i, \pi^i) \in \mathcal{V}$, for $i = 1, 2$, such that

$$(38a) \qquad -\mathbf{G}_0(x_1)\nabla_y\pi^i + \mu\mathrm{div}_y\left(\nabla_y w^i \mathbf{H}_0(x_1)\right) = \mathbf{G}_0(x_1)e_i \text{ in } Y_\mathcal{F},$$

$$(38b) \qquad \mathrm{div}_y(\mathbf{G}_0^T(x_1)w^i) = 0 \text{ in } Y_\mathcal{F},$$

where w^i and π^i are y-periodic, $w^i = 0$ on Y_Γ, and $\langle \pi^i \rangle_Y = 0$. For simplicity of notation, in the following we adopt a notation similar to that of section 3. We let $v = (w, \pi)$ be the solution and $\phi = (q, \zeta)$ be the test function. The bar $^-$ denotes an FE approximation. Then, (38) has the corresponding variational formulation. We wish to find $v \in \mathcal{V}$ such that

$$(39) \qquad \mathcal{A}_y(x_1)(v, \phi) = \int_{Y_\mathcal{F}} \mathbf{G}_0(x_1) : q\, dy \quad \forall\, \phi \in \mathcal{V},$$

where $\mathcal{A}_y(x_1)$ has the same form as (35).

It is useful to visualize the solutions. Fixing x_1, we solve the above variational form using $\mathbb{P}_2/\mathbb{P}_0$ Taylor–Hood finite elements over $Y_\mathcal{F}$. These elements satisfy the inf-sup stability conditions in Assumption 3.4; cf. [14]. We use quadratic elements for velocity and piecewise constants for pressure. In Figure 4, we plot the pressure π^1 and velocity w^1 cell solutions to (38), with right-hand-side $\mathbf{G}_0(x_1)e_1 = (1, 0)$, for $x_1 = 0, 1$ and $\alpha = 1/2$. We see that, as we move from $x_1 = 0$ to $x_1 = 1$, the tensor coefficients change. This, in turn, changes the pressure and velocity fields. As we stretch, the solid inclusion is thinner and has less of an effect on the flow in the horizontal direction. In the next section, we will compare the standard full solves ($h = 1/24$) to the hierarchical solve using our efficient algorithm.

Remark. It is important to note here that our inclusion has sharp corners. Near those regions, we will not be able to guarantee the solutions will be in our regularity space $\mathcal{U}$. However, since the data and other regions of the domain are smooth enough, this will not affect our results in a significant way.
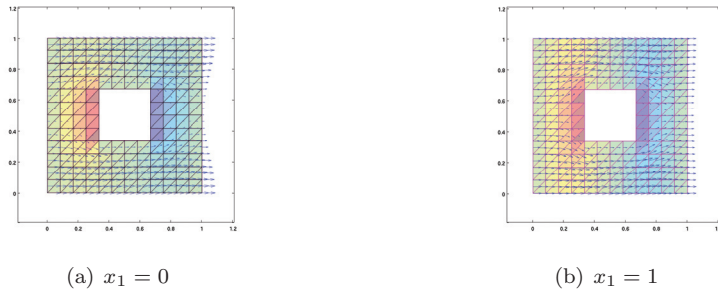
(a) $x_1 = 0$ (b) $x_1 = 1$

FIG. 4. *Pressure π^1 (triangle shading) and velocity w^1 (vectors) plots for $\alpha = 1/2$, $h = 1/12$ for* (a) $x_1 = 0$, (b) $x_1 = 1$ *in the periodic reference configuration.*
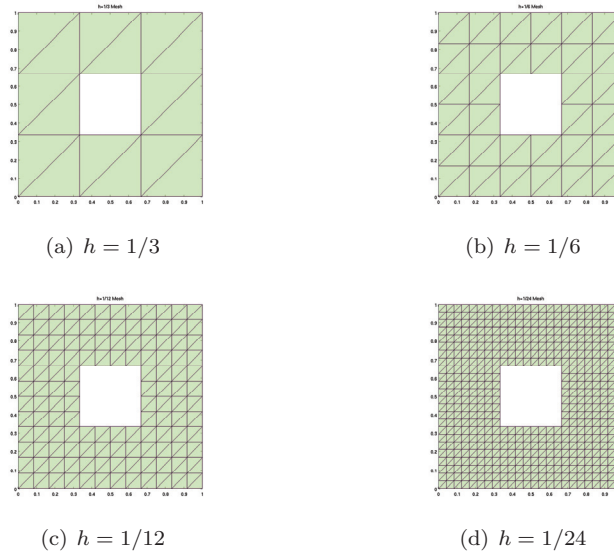

(a) $h = 1/3$ (b) $h = 1/6$

(c) $h = 1/12$ (d) $h = 1/24$

FIG. 5. *Four levels of meshes with coarsening factor $\kappa = 2$.*

5.2. Implementation of the algorithm. In this section, we implement the efficient hierarchical multiscale algorithm outlined in section 2.2. We apply these methods to (38). First, we build the nested sequence of FE spaces by coarsening the initial fine mesh in a structured way. From this sequence of meshes, we use $\mathbb{P}_2/\mathbb{P}_0$ Taylor–Hood elements to build the FE approximation spaces. Recall that the mapping (37) depends only on x_1, implying that the macrogrid need only vary in one direction. Hence, we construct a corresponding one-dimensional hierarchy of grids. Then, we implement the algorithm by computing the velocity. After averaging, we compute the modified permeability and compare our algorithm to the standard full solve at each point in our hierarchical grid.

With the intent of building our nested FE spaces, we begin with our meshes. We use the four meshes in Figure 5. We can view the generation of these meshes as either a coarsening of the finest mesh or a refinement of the coarsest mesh. A characteristic mesh size h is the length of the base of a triangular element (nonhypotenuse side). We
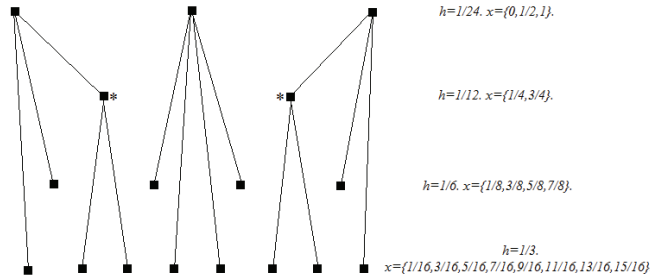
FIG. 6. *Schematic diagram of hierarchy of macrogrids and corresponding FE spaces. Stratification of spaces and lines indicates correction term relationships. The $*$ indicates where corrected solutions are used to correct once more.*

use these meshes to build a nested sequence of FE spaces. Using $\mathbb{P}_2/\mathbb{P}_0$ Taylor–Hood elements, where quadratics are used for velocity and constants for pressure, we denote the FE spaces as $\{\mathcal{V}_{3-l}\}_{l=0}^3$. Each space has the corresponding mesh size $h_l = 2^l(\frac{1}{24})$ for $l = 0, 1, 2, 3$ ($\kappa = 2$, FE coarsening factor). With these approximation spaces and using the notation in section 5.1, we will have the error estimate

$$\inf_{\phi \in \mathcal{V}_{3-l}} \|v - \phi\|_{\mathcal{V}} \le C\left(\frac{2^l}{24}\right)\|v\|_{\mathcal{U}}.$$

Remark. Here the Sobolev space $\mathcal{V}$ is given by (34), and the regularity space is given by $\mathcal{U} = (H^2_{\#,0}(Y_{\mathcal{F}}))^{d \times d} \times (H^1_{\int=0}(Y_{\mathcal{F}}))^d$. Note also that, since we are using quadratics for velocity, we will have an error estimate of h_l^2. However, due to using constant pressure, the overall estimate will be order h_l.

We now construct the nested macrogrids $\{\mathcal{T}_l\}_{l=0}^3 \subset [0,1]$ and subsequently the hierarchy of macrogrids $\{S_l\}_{l=0}^3$. Recall that our coarsening of the FE error is inversely proportional to the macro–grid spacing. With this in mind, we let $\mathcal{T}_0 = \{0, 1/2, 1\}$; then the initial grid spacing is $H2^0$, where is given by $H = 1/2$. The next macrogrids must have grid spacing $H2^{-l}$ for $l = 1, 2, 3,$. Thus, we have $\mathcal{T}_l = \{k/2^{l+1}\}_{k=0}^{2^{l+1}}$. We can now construct our hierarchy of grids S_l for $l = 0, 1, 2, 3$. Let the coarsest grid be $\mathcal{T}_0 = S_0 = \{0, 1/2, 1\}$; then $S_1 = \{1/4, 3/4\}$, $S_2 = \{(2k+1)/8\}_{k=0}^3$, and $S_3 = \{(2k+1)/16\}_{k=0}^7$. A schematic diagram of this hierarchy of grids and their relationship to the correction term procedure can be seen in Figure 6.

We implement the algorithm on the variational form (39) as follows. For $x' \in S_0 = \{0, 1/2, 1\}$, the so-called anchor points, we then solve for $v(x', \cdot) \in \mathcal{V}_3$ using the standard Galerkin FEM. We proceed to solve the lower level macrogrids by our inductive procedure. We use a simple 1-point interpolation to compute the correction term. For $x \in S_l$ and then for $x' \in (\cup_{k<l} S_k)$ we let

$$I_l^x(v) = v(x_1', \cdot)$$

be the macro–grid interpolation. For example, using $x' = 0 \in S_0$, we have computed $\bar{v}(0, \cdot) \in \mathcal{V}_3$ by the standard Galerkin FEM. We want to calculate $\bar{v}(1/4, \cdot)$, where $x = 1/4 \in S_1$. Using $I_1^{1/4}(\bar{v}) = \bar{v}(0, \cdot)$ as known data, we find the correction term
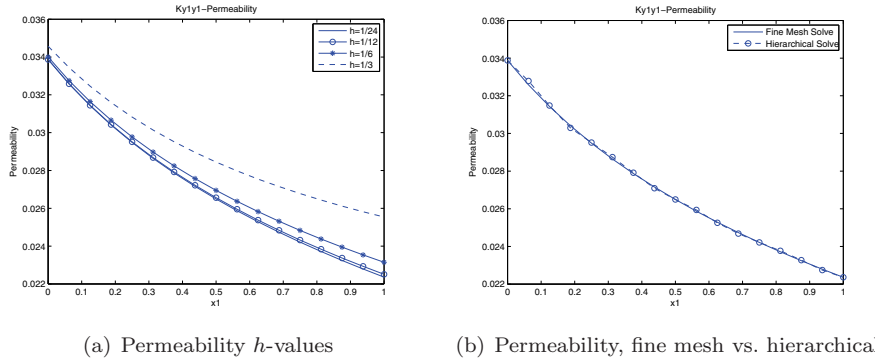
(a) Permeability h-values

(b) Permeability, fine mesh vs. hierarchical

FIG. 7. *Interpolated permeability values for $x_1^i = i/16$, $i = 0, \ldots, 16$, with $\alpha = 1/2$. (a) Varying $h = 1/3, 1/6, 1/12, 1/24$, (b) hierarchical solve "- o -" vs. fine mesh solve "——."*

$\bar{v}_c(1/4, \cdot) \in \mathcal{V}_2$ such that

$$\mathcal{A}_y(1/4)(\bar{v}_c, \phi) = \int_{Y_{\mathcal{F}}} \mathbf{G}_0(1/4) : q\,dy - \mathcal{A}_y(1/4)(\bar{v}(0, \cdot), \phi)$$

for all $\phi \in \mathcal{V}_2$. We write the solution at $x = 1/4$ as

$$\bar{v}(1/4, \cdot) = \bar{v}_c(1/4, \cdot) + \bar{v}(0, \cdot).$$

We continue this procedure. For $x = 3/4$, we use $I_1^{3/4}(\bar{v}) = \bar{v}(1, \cdot)$ as known data as above. Since $x = 3/4 \in S_1$, we solve for $\bar{v}_c \in \mathcal{V}_2$ and write $\bar{v}(3/4, \cdot) = \bar{v}_c(3/4, \cdot) + \bar{v}(1, \cdot)$. Continuing on in this manner, we use the corrected solution $\bar{v}(1/4, \cdot)$ to compute the correction terms at $x = 3/16, 5/16$ in $\mathcal{V}_0$. We also use the corrected solution $\bar{v}(3/4, \cdot)$ to compute the correction terms at $x = 11/16, 13/16$ in $\mathcal{V}_0$. Indeed, using $\bar{v}(0, \cdot)$, we build the correction terms at $x = 1/8$ in $\mathcal{V}_1$ and at $x = 1/16$ in $\mathcal{V}_0$. Using $\bar{v}(1/2, \cdot)$, we build the correction terms at $x = 3/8, 5/8$ in $\mathcal{V}_1$ and at $x = 7/16, 9/16$ in $\mathcal{V}_0$. Finally, using $\bar{v}(1, \cdot)$, we build the correction terms at $x = 7/8$ in $\mathcal{V}_1$ and at $x = 15/16$ in $\mathcal{V}_0$. In this way, we build all solutions in $\mathcal{T}_3 = \{k/16\}_{k=0}^{16}$. We summarize this procedure in Figure 6.

We compute the solutions to cell equations (38) for $i = 1$. First, we compare the convergence results for standard solves, for varying h_l-values. We then compare the convergence results for the finest mesh standard Galerkin solve to the implementation of our efficient algorithm (hierarchical solve). To this end, we define the modified permeability in the y_1 direction as

$$(40) \qquad\qquad K_{y_1 y_1}(x_1) = \int_{Y_{\mathcal{F}}} w^1(x_1, y)\,dy,$$

where $w^1(x_1, y)$ is the y_1 component of the velocity in (38) for $i = 1$. Ultimately, we want to compute permeability, so this is a reasonable measure of accuracy.

In Figures 7 and 8, we present a summary of our results. In Figure 7, we let $\alpha = 1/2$, where the mapping (37) is weak. Using the standard Galerkin FEM for the macropoints $\mathcal{T}_3 = \{k/16\}_{k=0}^{16}$, in Figure 7(a), we compute modified permeabilities in the y_1 direction (40) for varying values of h_l. Then, we interpolate the values to make the trends clearer. Since the mapping is weak, the solution changes very slowly and

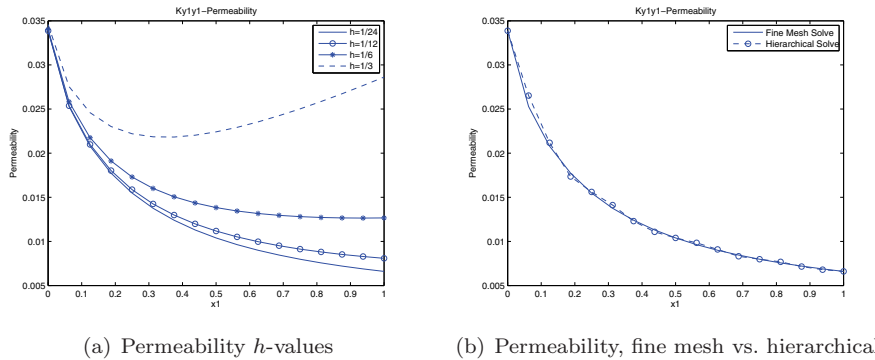(a) Permeability h-values   (b) Permeability, fine mesh vs. hierarchical

FIG. 8. *Interpolated permeability values for $x_1^i = i/16$, $i = 0, \ldots, 16$, with $\alpha = 5$. (a) Varying $h = 1/3, 1/6, 1/12, 1/24$; (b) hierarchical solve "- ○ -" vs. fine mesh solve "—."*

not much is gained from decreasing h_l past a certain value. In Figure 7(b), we compare our efficient algorithm described above with the finest mesh solution $h = 1/24$, used at all points in $\mathcal{T}_3$. We see that we obtain the same order of accuracy using the standard solve as with our efficient hierarchical algorithm.

In Figure 8, we proceed exactly as in Figure 7, but we let $\alpha = 5$. This corresponds to a strong stretch. In this case, the microstructure varies greatly. We observe that as we move to the right of the domain, the deformation from our mapping is greatest. Using the standard Galerkin FEM, we observe strong errors in Figure 8(a) when larger values of h_l are used. Comparing the standard solve with $h = 1/6$ to the standard solve $h = 1/24$, we observe very large errors at $x_1 = 1$. In Figure 8(b), we again compare our efficient algorithm to the standard solve with the finest mesh $h = 1/24$. We observe that we obtain the same order of accuracy. Moreover, we observe good convergence in the right-hand side of the domain with our hierarchical solve.

Note that we observe low-frequency errors because of the one-dimensional macrogrid used in Figure 6. For example, at $x_1 = 1/8$ ($h = 1/6$), we correct with the solution at $x_1 = 0$ ($h = 1/24$), from the left, while at $x_1 = 3/8$ ($h = 1/6$), we correct with the solution at $x_1 = 1/2$ ($h = 1/24$), from the right. This causes the low-frequency errors in the permeability. To correct this, one may use a higher order interpolation. For example, one may use a higher order interpolation on the right-hand side to correct the solution, i.e.,

$$I_2^{1/8}(\bar{v}) = \frac{1}{2}\left(\bar{v}(0, \cdot) + \bar{v}\left(\frac{1}{2}, \cdot\right)\right).$$

These options will be explored in future work. The two examples serve as a "proof of concept" and demonstrate that the algorithm can be simply implemented and is the same order of accuracy as the standard full solve.

6. Conclusions. We developed an efficient multiscale FEM for computing effective coefficients in a medium with a slowly varying microstructure. We outlined a general framework for building a dense hierarchy of macrogrids and a corresponding nested sequence of approximation spaces. We applied our abstract framework to computing the effective permeability of the Stokes equations in a slowly varying porous medium that is obtained from a periodic domain by a smooth map. For a dense hierarchy of different levels of macroscopic points, we obtained an accuracy for

the effective permeability essentially equal to that for the full solve, with essentially the same number of degrees of freedom as for solving a single cell problem. This was achieved by considering the modified Stokes equations, more precisely, the ALE formulation in the periodic domain. Using the ALE formulation, the general algorithm framework can then be applied. Cell problems were solved with different levels of resolution depending on the level of macrogrid. Those macroscopic points at the lower (sparser) levels in the hierarchy are solved more accurately, while points at the higher (denser) levels are solved less accurately. Solutions for neighboring points at the lower levels, which are solved with higher accuracy, are used to correct the finite element error. Finally, a numerical example is implemented to demonstrate the algorithm. To this end, a component of the permeability is compared. The full solve is compared to the efficient hierarchical solve. The same order of accuracy is observed.

7. Appendix: Two-scale expansion in the ALE formulation. In this appendix, we apply the method of two-scale asymptotic expansion as in [20] to the modified Stokes operator $\mathcal{L}_\varepsilon\left(x, \frac{x}{\varepsilon}\right)$ given by (30). Recall that these equations are presented in the periodic reference domain Ω. This is the so-called ALE formulation of the Stokes equations; cf. [13]. From this procedure, we obtain modified cell and homogenized operators $\mathcal{L}_y(x)$ and $\mathcal{L}(x)$, respectively.

To this end, we let $y = x/\varepsilon$, and thus derivatives transform as $\nabla \to \nabla_x + \frac{1}{\varepsilon}\nabla_y$. In addition, assume the following ansatz for the deformation $\widetilde{\mathbf{x}}_\varepsilon(x)$:

$$\tag{41} \widetilde{\mathbf{x}}_\varepsilon(x) = \widetilde{\mathbf{x}}_0(x) + \varepsilon\widetilde{\mathbf{x}}_1(x, y).$$

We assume the regularities $\widetilde{\mathbf{x}}_0 \in C^2(\bar{\Omega})$ and $\widetilde{\mathbf{x}}_1(x, y) \in C^2(\bar{\Omega} \times Y)$, and thus $\widetilde{\mathbf{x}}_\varepsilon(x) \in C^2(\bar{\Omega})$.

Remark. This ansatz is reasonable for many applications; cf. [19]. Essentially, the mapping has a large macroscopic part and a small oscillatory correction. In the context of FSI, we have some macroscopic deformation over the whole domain and some small pore-scale deformation throughout.

We expand the gradient, Jacobian, and related tensors as

$$\tag{42} \mathbf{F}_\varepsilon(x) = (\nabla_x\widetilde{\mathbf{x}}_0(x) + \nabla_y\widetilde{\mathbf{x}}_1(x, y)) + \varepsilon(\nabla_x\widetilde{\mathbf{x}}_1(x, y)) = \mathbf{F}_0(x, y) + \varepsilon\mathbf{F}_1(x, y),$$

and

(43a)
$$\mathbf{G}_\varepsilon(x) = \mathbf{G}_0(x, y) + \varepsilon\mathbf{G}_1(x, y) + \cdots, \qquad \mathbf{H}_\varepsilon(x) = \mathbf{H}_0(x, y) + \varepsilon\mathbf{H}_1(x, y) + \cdots,$$
(43b)
$$J_\varepsilon(x) = J_0(x, y) + \varepsilon J_1(x, y) + \cdots.$$

Here, the functions J_i, $\mathbf{F}_i$, $\mathbf{G}_i$, and $\mathbf{H}_i$ are y-periodic for $i = 0, 1, \ldots$.

Remark. To ensure that we have a meaningful deformation, we assume the nondegeneracy condition. There exists a c such that

$$\tag{44} J_\varepsilon(x) > c > 0 \quad \text{and} \quad J_0(x, y) > c > 0 \quad \forall x \in \Omega.$$

In addition, $\mathbf{F}_0(x, y)$ is of class C^1 and therefore bounded. Hence, there exists c such that

$$\tag{45} \left\|\mathbf{F}_0^{-T}(x, y)\right\| > c > 0 \quad \forall x \in \Omega.$$

These bounds will ensure a well-posed modified Stokes problem.

We expand velocity and pressure as in the case of slowly varying media (3):

(46a) $$v_\varepsilon(x) = \varepsilon^2 \left(v_0(x,y) + \varepsilon v_1(x,y) + \cdots \right),$$

(46b) $$p_\varepsilon(x) = p_0(x) + \varepsilon p_1(x,y) + \cdots .$$

Using the above two-scale expansions (42)–(46), we can write the momentum equation (30a) as

$$- \left(\mathrm{div}_x + \frac{1}{\varepsilon}\mathrm{div}_y \right) \left((p_0(x) + \varepsilon p_1(x,y) \cdots) \left(\mathbf{G}_0(x,y) + \varepsilon \mathbf{G}_1(x,y) + \cdots \right) \right)$$

$$+ \mu \left(\mathrm{div}_x + \frac{1}{\varepsilon}\mathrm{div}_y \right) \left[\left(\left(\nabla_x + \frac{1}{\varepsilon}\nabla_y \right) \left(\varepsilon^2 v_0(x,y) + \varepsilon^3 v_1(x,y) \cdots \right) \right) \right.$$

$$\left. \times \left(\mathbf{H}_0(x,y) + \varepsilon \mathbf{H}_1(x,y) + \cdots \right) \right] = f(x) \left(J_0(x,y) + \varepsilon J_1(x,y) \cdots \right),$$

and for the conservation of mass equation (30b)

$$\left(\mathrm{div}_x + \frac{1}{\varepsilon}\mathrm{div}_y \right) \left(\left(\mathbf{G}_0^T(x,y) + \varepsilon \mathbf{G}_1^T(x,y) + \cdots \right) \left(\varepsilon^2 v_0(x,y) + \cdots \right) \right) = 0.$$

Collecting the ε^0 terms from the conservation of momentum, we have

$$-\mathrm{div}_x \left(p_0(x)\mathbf{G}_0(x,y) \right) - \mathrm{div}_y(p_0(x)\mathbf{G}_1(x,y)) - \mathrm{div}_y(p_1(x,y)\mathbf{G}_0(x,y))$$

(47) $$+ \mu \mathrm{div}_y \left(\nabla_y v_0(x,y)\mathbf{H}_0(x,y) \right) = f(x)J_0(x,y),$$

and for the ε^1 terms from the conservation of mass equation

(48) $$\mathrm{div}_y \left(\mathbf{G}_0^T(x,y)v_0(x,y) \right) = 0.$$

We may simplify (47) by noting that Piola transform $\mathbf{G}_\varepsilon(x)$ is divergence-free via the identity

$$\int_{\mathcal{P}_\varepsilon} \mathrm{div}_x(\mathbf{G}_\varepsilon(x))dx = \int_{\partial\mathcal{P}_\varepsilon} \mathbf{G}_\varepsilon(x) \cdot n(x)dx$$

$$= \int_{\partial\widetilde{\mathcal{P}}_\varepsilon} \mathbf{I} \cdot \widetilde{n}(\tilde{x})d\tilde{x} = \int_{\widetilde{\mathcal{P}}_\varepsilon} \mathrm{div}_{\tilde{x}}(\mathbf{I})d\tilde{x} = 0.$$

From here, we see that the tensor $\mathbf{G}_\varepsilon(x)$ satisfies $\mathrm{div}_x(\mathbf{G}_\varepsilon(x)) = 0$. Using the asymptotic expansions (43a), we obtain

$$\left(\mathrm{div}_x + \frac{1}{\varepsilon}\mathrm{div}_y \right) \left(\mathbf{G}_0(x,y) + \varepsilon \mathbf{G}_1(x,y) + \cdots \right) = 0.$$

Gathering similar terms in ε, we see that for ε^{-1}

$$\mathrm{div}_y(\mathbf{G}_0(x,y)) = 0,$$

and for ε^0

$$\mathrm{div}_x(\mathbf{G}_0(x,y)) + \mathrm{div}_y(\mathbf{G}_1(x,y)) = 0.$$

Using these identities, we deduce that

$$-\text{div}_x(p_0(x)\mathbf{G}_0(x,y)) - \text{div}_y(p_0(x)\mathbf{G}_1(x,y)) - \text{div}_y(p_1(x,y)\mathbf{G}_0(x,y))$$
$$= -\mathbf{G}_0(x,y)\nabla_x p_0(x) - \mathbf{G}_0(x,y)\nabla_y p_1(x,y).$$

Using the above identity, we simplify (47) along with the incompressibility equation (48). We write the cell problem for the modified Stokes equations in the periodic fluid cell $Y_\mathcal{F}$ as

$$-\mathbf{G}_0(x,y)\nabla_y p_1(x,y) + \mu\text{div}_y(\nabla_y v_0(x,y)\mathbf{H}_0(x,y)) = \mathbf{G}_0(x,y)\nabla_x p_0(x) + f(x)J_0(x,y),$$
$$\text{div}_y(\mathbf{G}_0^T(x,y)v_0(x,y)) = 0,$$

where v_0 and p_1 are y-periodic, $v_0 = 0$ on Y_Γ, and $\langle p_1\rangle_Y = 0$. Note that the right-hand side of the above problem contains components that depend on the fast variable y, unlike in the slowly varying case in section 2.1. Indeed, we let

$$(49a) \qquad\qquad v_0(x,y) = w_1(x,y)\nabla_x p_0(x) + w_2(x,y)f(x),$$
$$(49b) \qquad\qquad p_1(x,y) = \pi_1(x,y)\nabla_x p_0(x) + \pi_2(x,y)f(x),$$

where $(w_j^i(x,y), \pi_j^i(x,y))$, $i = 1,\ldots,d$, are the solutions to the modified Stokes cell equations

$$-\mathbf{G}_0\nabla_y\pi_1^i + \mu\text{div}_y\left(\nabla_y w_1^i\mathbf{H}_0\right) = \mathbf{G}_0 e_i \text{ in } Y_\mathcal{F},$$
$$\text{div}_y(\mathbf{G}_0^T w_1^i) = 0 \text{ in } Y_\mathcal{F},$$

and for the second cell

$$-\mathbf{G}_0\nabla_y\pi_2^i + \mu\text{div}_y\left(\nabla_y w_2^i\mathbf{H}_0\right) = J_0 e_i \text{ in } Y_\mathcal{F},$$
$$\text{div}_y(\mathbf{G}_0^T w_2^i) = 0 \text{ in } Y_\mathcal{F},$$

where w_j^i and π_j^i are y-periodic, $w_j^i = 0$ on Y_Γ, and $\langle\pi_j^i\rangle_Y = 0$. The above equations are the modified Stokes cell operator $\mathcal{L}_y(x)$ with differing right-hand-side data. Taking the next term in the two-scale expansion of (30b), we have

$$\text{div}_x(\mathbf{G}_0^T(x,y)v_0(x,y)) + \text{div}_y(\mathbf{G}_1^T(x,y)v_0(x,y)) + \text{div}_y(\mathbf{G}_0^T(x,y)v_1(x,y)) = 0.$$

Taking the average over the unit cell, using y-periodicity, $v_\varepsilon(x,y) = 0$ on Γ_ε, and the divergence theorem, the div_y terms vanish. We obtain the homogenized operator $\mathcal{L}(x)$ in the periodic reference domain

$$\text{div}_x\left(\langle\mathbf{G}_0^T(x,y)v_0(x,y)\rangle_Y\right) = 0 \text{ in } \Omega.$$

Using the relation (49), we see that

$$\text{div}_x\left(\langle\mathbf{G}_0^T(x,y)w_1(x,y)\rangle_Y\nabla_x p_0(x)\right) + \text{div}_x\left(\langle\mathbf{G}_0^T(x,y)w_2(x,y)\rangle_Y f(x)\right) = 0.$$

Letting

$$\mathbf{K}(x) = \langle\mathbf{G}_0^T(x,y)w_1(x,y)\rangle_Y \quad\text{and}\quad \bar{f}(x) = \langle\mathbf{G}_0^T(x,y)w_2(x,y)\rangle_Y f(x),$$

we write this effective homogenized equation as

$$\text{div}_x\left(\mathbf{K}(x)\nabla_x p_0(x) + \bar{f}(x)\right) = 0 \text{ in } \Omega.$$

Here, we may make comparisons parallel to Darcy law (9). We have the x-dependent modified permeability $\mathbf{K}(x)$ and the modified Darcy velocity $\xi = \mathbf{K}(x)\nabla_x p_0(x) + \bar{f}(x)$. We also require the boundary conditions $\xi \cdot \nu = 0$ on $\partial\Omega$, where ν is the unit normal.

Remark. Note here that if our mapping is the identity, that is, $\widetilde{\mathbf{x}}_\varepsilon(x) = x$, all the related tensors are the identity matrix. In this case, we observe that the equations are the same as the purely periodic setting.

Acknowledgment. We would like to thank Juan Galvis for allowing us to use his finite element library and for the useful discussion on implementation of this work.

REFERENCES

[1] A. Abdulle, W. E, B. Engquist, and E. Vanden-Eijnden, *The heterogeneous multiscale method*, Acta Numer., 21 (2012), pp. 1–87.

[2] G. Allaire, *Homogenization and two-scale convergence*, SIAM J. Math. Anal., 23 (1992), pp. 1482–1518.

[3] C. Amrouche and V. Girault, *On the existence and regularity of the solution of Stokes problem in arbitrary dimension*, Proc. Japan Acad. Ser. A Math. Sci., 67 (1991), pp. 171–175.

[4] S. C. Brenner and R. S. Scott, *The Mathematical Theory of Finite Element Methods*, Texts Appl. Math. 15, Springer, New York, 2008.

[5] F. Brezzi and M. Fortin, *Mixed and Hybrid Finite Element Methods*, Springer, New York, 1991.

[6] D. L. Brown, *Multiscale Methods for Fluid-Structure Interaction*, Ph.D. thesis, Texas A&M University, College Station, TX, 2012.

[7] D. L. Brown, P. Popov, and Y. Efendiev, *On homogenization of Stokes flow in slowly varying media with applications to fluid-structure interaction*, GEM Int. J. Geomath., 2 (2011), pp. 281–305.

[8] H. Darcy, *Les fontaines publique de la ville de Dijon*, Librairie des Corps Impériaux des Ponts et Chaussées et des Mines, Paris, 1856.

[9] H. I. Ene, *Modeling the flow through porous media*, in Emerging Technologies and Techniques in Porous Media, Kluwer Academic Publishers, Dordrecht, The Netherlands, 2004.

[10] H. I. Ene and E. Sanchez-Palencia, *Equations et phénomènes de surface pour l'écoulement dans un modèle de milieu poreux*, J. Mécanique, 14 (1975), pp. 73–108.

[11] A. Ern and J. L. Guermond, *Theory and Practice of Finite Elements*, Appl. Math. Sci. 159, Springer, New York, 2004.

[12] L. Formaggia, A. Quarteroni, and A. Veneziani, *Cardiovascular Mathematics: Modeling and Simulation of the Circulatory System*, Modeling, Simulation & Applications, Springer, Milan, 2009.

[13] G. P. Galdi and R. Rannacher, *Fundamental Trends in Fluid-Structure Interaction*, Contemporary Challenges in Mathematical Fluid Dynamics and Its Applications 1, World Scientific, Singapore, 2010.

[14] V. Girault and P. A. Raviart, *Finite Element Methods for Navier-Stokes Equations*, Springer, Berlin, 1986.

[15] V. H. Hoang and C. Schwab, *High-dimensional finite elements for elliptic problems with multiple scales*, Multiscale Model. Simul., 3 (2005), pp. 168–194.

[16] A. Mikelic, *Homogenization theory and applications to filtration through porous media*, in Filtration in Porous Media and Industrial Application, Lecture Notes in Math. 1734, A. Fasano, ed., Springer, Berlin, 2000, pp. 127–214.

[17] M. A. Peter, *Homogenisation in domains with evolving microstructure*, C. R. Mécanique, 335 (2007), pp. 357–362.

[18] M. A. Peter, *Homogenisation of a chemical degradation mechanism inducing an evolving microstructure*, C. R. Mécanique, 335 (2007), pp. 679–684.

[19] P. Popov, Y. Gorb, and Y. Efendiev, *Iterative upscaling of flows in deformable porous media*, submitted.

[20] E. Sanchez-Palencia, *Non-homogeneous Media and Vibration Theory*, Lecture Notes in Phys. 127, Springer, Berlin, 1980.

[21] R. Temam, *Navier-Stokes Equations: Theory and Numerical Analysis*, North–Holland, Amsterdam, New York, Oxford, UK, 1977.